R & M No. 3841

R & M No. 3841

PROCUREMENT EXECUTIVE, MINISTRY OF DEFENCE

Aeronautical Research Council
Reports and Memoranda

THE RESONANCE FREQUENCIES OF VENTILATED WIND TUNNELS

by

D.G. Mabey

Structures Department, RAE Farnborough

London: Her Majesty's Stationery Office

£8 NET

UDC 533.6.071.3 : 533.6.071.11 : 621.532.1 : 534.242 : 534.63

THE RESONANCE FREQUENCIES OF VENTILATED WIND TUNNELS

By D. G. Mabey

Structures Department, RAE Farnborough

REPORTS AND MEMORANDA No.3841*

April 1978

SUMMARY

Experiments suggest that the theory widely used to predict the transverse resonance frequencies in slotted tunnels is in error in the Mach number range from 0 to 0.5. One reason for the error is that the theory is based on an unrepresentative wall boundary condition. Moreover, the theory implies that the plenum chamber surrounding the working section is large, whereas the plenum chamber depth is generally less than twice the tunnel height.

An improved theory is developed, which shows that the resonance frequencies of ventilated tunnels are influenced by the depth of the plenum chamber for Mach numbers up to about M = 0.6. Although the theory is approximate, it agrees well with experiments for slotted and perforated walls (with both normal and 60° inclined holes).

The results are consistent with other experiments which show that plenum chamber design can influence the flow unsteadiness within the working section of a ventilated tunnel.

* Replaces RAE Technical Report 78038 - ARC 37974

LIST OF CONTENTS

1 INTRODUCTION

There is considerable current interest in the use of wind tunnels for dynamic experiments (such as the measurement of flutter boundaries, unsteady control surface characteristics or rigid-body derivatives) at subsonic and transonic speeds. Such measurements may be in error if the test frequency coincides with a transverse resonance frequency in the tunnel working section, for then the aerodynamic force may be utterly inappropriate to unconfined flow[1]. The results of such a coincidence in frequencies could vitiate the flutter testing of an aeroelastic model. In addition, if any aerodynamic excitation coincides with a resonance frequency, excessive flow unsteadiness might develop in the working section. This unsteadiness could hinder all dynamic measurements at this frequency[2]. Hence it is important that the tunnel transverse resonance frequencies should be correctly predicted.

A recent experiment[3] in which resonances were excited by the vortices shed from circular cylinders in closed and slotted working sections suggested that Acum's theory for slotted tunnels[4] was seriously in error in the Mach number range up to $M = 0.5$. We shall see in section 2 that this error arose from the use of an unrepresentative boundary condition for the slotted wall. New experiments confirm that there is an important influence of plenum chamber size. Fig 1a shows some typical results for three depths of plenum chamber and a wide range of slot configurations, in comparison with the theoretical curve against slot parameter in the special case $M = 0$. The first mode frequencies for a shallow plenum chamber are much lower than the predicted value from Ref 4, and fall still further as the plenum chamber depth increases.

Therefore an approximate theory for ventilated tunnels has been developed, which predicts the resonance frequencies as a function of the free stream Mach number M, the plenum chamber depth, d, and either a slot geometry factor, F, or a wall porosity factor $2kT/H$ suitable for ventilated tunnels in general. Fig 1b shows that the new theory does correctly predict the measured frequencies for the slotted working sections considered at $M = 0$. The new theory covers both slotted and perforated working sections, whereas the earlier theory was only valid for slotted working sections.

The main predictions have been confirmed by experiments in a small pilot wind tunnel (100 mm × 100 mm) with slotted and perforated walls. Sections 2 and 5 highlight the most interesting features of this paper.

2 OUTLINE OF THEORY

The previous theory for the resonance frequencies[4] assumed that the oscillatory pressure difference across the equivalent homogeneous wall (which replaced the slotted wall) was independent of the plenum chamber size and proportional to the streamline curvature. Mathematically, this condition on ϕ_x and ϕ_{xz} was integrated to give (Ref 4, equation (22)) the following relation between the velocity potential, ϕ, and its derivative normal to the wall, ϕ_z :

$$\phi \pm \tfrac{1}{2}(FH\phi_z) = 0 , \tag{1}$$

where the slot parameter $F = (2a/\pi H) \ln [\operatorname{cosec} (\pi b/2a)]$,
and a , b and H are respectively slot spacing, slot width and tunnel height.

With this condition the solution for the resonance frequencies was given by the eigensolution

$$\tan p + Fp = 0 , \tag{2}$$

for p , a non-dimensional wave number normal to the wall (Appendix, equations (A-15) and (A-27)). Thus the resonance frequencies varied with the slot parameter from the closed ($F = \infty$, $p = \pi/2$) to the open ($F = 0$, $p = \pi$) organ-pipe values.

For unsteady flow equation (1) should be replaced by the differential equation (Ref 5, equation (4-4))

$$\phi_x + \phi_t/U \pm \tfrac{1}{2}(FH\phi_{xz}) = 0 . \tag{3}$$

With this condition equation (2) is replaced by

$$\tan p + M^2 Fp = 0 . \tag{4}$$

(This may be seen by putting $g = 0$ in equation (A-29).)

Equation (4) predicts that at $M = 0$ the resonance frequencies are equal to the open organ-pipe values, independent of the slot parameter F ; this prediction is unrealistic. In contrast, at $M = 1$, equation (2) is recovered.

Now the slot parameter, F , was derived by Davis and Moore[6] from the potential flow through a grid, originally given by Lamb[7]. Lamb used this solution to investigate the diffraction of sound through a grid in air at rest. He found that when the wavelength of the incident sound was long relative to the slot width,

a large proportion of sound was diffracted through the grid; for example for a rectangular grid with a slot width of only 10% open area ratio (typical of many slotted tunnels), 88% of the incident sound is transmitted and only 12% reflected. With such a large proportion of the incident sound passing through the grid it is surely unwise to neglect the finite size of the plenum chamber of a ventilated tunnel, at least at low speeds.

The new theory includes a plenum chamber and uses the notation shown in Fig 2; the full analysis is given in the Appendix. Let us first consider the steady flow. The two-dimensional working section extends from $x = -\infty$ to $+\infty$ and has a uniform flow of velocity U at a Mach number M. It is surrounded by two plenum chambers, each of depth $dH/2$, with zero mean flow. The working section is separated from the plenum chambers by homogeneous ventilated walls, which are thin, rigid and have no boundary layers. For simplicity, we assume that the mean pressure and static temperature are the same in the working section and the plenum chambers. Hence the densities in the free stream and the plenum chambers are the same. However, we know from the measurements of Smith and Shaw[8] that the static temperature within a cavity is close to the free-stream total temperature, not the free-stream static temperature; but the error in density is trivial at Mach numbers up to $M = 1.0$.

For the oscillatory flow we seek compatible solutions for the velocity potentials ϕ and ψ in the free-stream and plenum chambers. The boundary condition on the outer walls of the plenum chamber is a potential flow one - simply that the normal velocity should be zero. Thus

$$\psi_z = 0 \quad \text{on} \quad y = \pm H(1 + d)/2 \quad . \tag{5}$$

The specification of boundary conditions on the inner walls of the plenum chamber is controversial. We will assume that there is continuity of mass flow from the working-section to the plenum chamber, so that

$$\phi_z = \psi_z \quad , \quad \text{on} \quad y = \pm H/2 \quad . \tag{6}$$

In addition, different expressions are developed in the Appendix for the pressure drop across perforated and slotted walls.

For perforated walls of thickness Z, we note that with a single normal hole of diameter D and air at rest, a phase lag of 90° between the applied pressure and the normal velocity is both predicted and measured[9]. In accord with

a recent theoretical study[10], we assume that the free-stream flow does not alter this relationship and that the hole resistance remains much smaller than the impedance. The pressure drop across a single hole is then generalised to predict the pressure drop across perforated walls at $z = \pm H/2$ containing many holes to give equation (A-12), viz

$$\phi_x + (\phi_t - \psi_t)/U \pm (ik\omega T/U)\phi_z = 0 \quad , \tag{7}$$

where, as in equation (A-11), $k = (1 - \sigma)/\sigma$ is an empirical function of the open area ratio σ, ω is the circular frequency of the oscillations, and the effective hole diameter is

$$T = 0.85D + Z \quad . \tag{8}$$

For slotted walls we assume that the steady-flow value of F is still valid for the oscillatory flow and hence derive the wall condition in equation (A-13) viz:

$$\phi_x + (\phi_t - \psi_t)/U \pm (FH/2)\phi_{xz} = 0 \quad . \tag{9}$$

Although equations (7) and (9) look quite different, they predict similar trends for the influence of plenum chamber depth, wall porosity and Mach number on the resonance frequencies. Hence they may be regarded as different versions of Bernoulli's equation for the oscillatory flow through an orifice or a slot (Ref 11, equation 11.3.37).

With these boundary conditions, eigenvalues, p, can be calculated. At low speeds ($0 < M < 0.5$) the resonance frequencies in perforated and slotted tunnels are roughly constant and remain slightly below the closed/closed organ-pipe frequencies at $M = 0$ with a tunnel of height $H(1 + d)$. From $M = 0.5$ to 0.7 the resonance frequencies increase rapidly and the influence of the plenum chamber becomes negligible. At the special Mach number, $M = (\sqrt{5} - 1)/2 = 0.618$, from equations (A-25) and (A-26), the resonance frequencies of perforated and slotted tunnels are identical, independent of the plenum chamber depth and the

wall porosity, and equal to the closed tunnel values ($p = 0.5\pi$) and the form of the solution changes. From $M = 0.7$ to 1.0 the resonance frequencies fall monotonically and are virtually unaffected by the depth of the plenum chamber. These predictions were unexpected (see sketch in Fig 2) but we shall see that they are broadly confirmed by the experiments.

Acoustic theory may be invoked to explain the surprising change in the character of the solutions at $M = 0.618$. Fig 3 compares what would happen at the closed and open portions of the walls of a two-dimensional slotted tunnel with an oscillating model on the centre line. (The notation follows Ref 11, Figs 11.2 to 11.5). Fig 3a identifies the single incident pressure wave which would be directly reflected onto the model from the closed portions of the boundary. When the time taken for the journey to and from the model

$$t = HM/U\sqrt{1 - M^2} \quad ,$$

is the half period, $1/(2f)$, the reflected wave will cancel the source wave and resonance will occur. Thus the first resonance frequency in a fully closed tunnel is

$$f = U\sqrt{1 - M^2}/(2HM) \quad , \quad ie \quad p = \pi/2 \quad , \tag{10}$$

as previously given by Acum[4]. In contrast, Fig 3b shows that for the open portions of the boundary, acoustic theory would impose conditions analogous to Snell's law of refraction in optics. The boundary between the free-stream flow and the static air in the plenum chamber is assumed to deflect as pressure waves from the model intersect it (see Ref 11, p 705). From Fig 3a, the inclination of the wave front to the boundary, ϕ_1, must increase with speed according to the relation

$$\cos \phi_1 = - M \quad . \tag{11}$$

With our assumption of a uniform static temperature across the free stream and the plenum chamber the velocity of sound is uniform across the tunnel. Hence the inclination of the refracted wave front in the plenum chamber must satisfy the condition

$$\cos \phi_2 = (\cos \phi_1)/(1 + M \cos \phi_1) \quad , \tag{12}$$

based on Ref 11, equation (11.1.17).

The limiting case

$$\phi_2 = 180^\circ \text{ , } \cos \phi_1 = -1/(1 + M) \text{ ,} \tag{13}$$

defines a value of ϕ_1 above which sound waves would not enter the plenum chamber. Manifestly, at this condition the resonance frequencies would not be influenced by the open area ratio nor by the depth of the plenum chamber. The critical speed for this condition is given by equations (11) and (13) as

$$\cos \phi_1 = -M = -1/(1 + M) \text{ ,}$$

or

$$M^2 + M - 1 = 0 \text{ .} \tag{14}$$

Equation (14) has the solution

$$M = (\sqrt{5} - 1)/2 = 0.618 \text{ ,} \tag{15}$$

precisely the critical speed found in the Appendix.

This argument rests on the assumption of a travelling wave along the equivalent homogeneous wall. The concept of a continuously varying boundary displacement is easier to accept for a narrow slot than for a succession of individual perforations. Nevertheless, it provides an interesting physical explanation of what the theory predicts and the experiments confirm in both slotted and perforated working sections.

It is important to note that the solutions for perforated and slotted tunnels differ appreciably in the limit at $M = 0$. Considering first only the odd eigenvalues, we find in equation (A-48) that for perforated walls:

$$\tan p - \cot(dp) + (2kT/H)p = 0 \text{ ,} \tag{16}$$

so that the resonance frequencies are influenced by the wall parameter, as well as the plenum chamber depth. When the perforated walls are removed, $k = 0$ and the solution of equation (16) is then

$$p = n\pi/2(1 + d) \text{ ,} \tag{17}$$

where $n = 1, 3, 5,$ etc which we recognise as the odd eigenvalues for the closed

organ pipe of height $(1 + d)H$. In contrast, in equation (A-1) for slotted tunnels we find for all finite values of F

$$\tan p \tan (dp) = 1 \quad . \tag{18}$$

The solution of equation (18) is also equation (17). Hence equation (16) must be regarded as more realistic than equation (15), and as reflecting adversely on the boundary condition expressed by equation (9). Now there is no *a priori* reason why the oscillatory flow through an orifice should differ in character from that through a slot at $M = 0$. Hence, when calculating resonance frequencies, it is considered better to replace a slotted wall by a perforated wall of the same open area ratio, and some equivalent hole size. Our experiments in relation to equation (8) suggest that the hole diameter D may be replaced by the slot width b so that

$$T = 0.85b + Z \quad , \tag{19}$$

where Z is now the depth of the slat, instead of the plate thickness of the perforated wall. Fig 1b shows that this approximation works well for slotted walls in the range of wall parameters of interest ($2kT/H < 0.5$).

3 EXPERIMENTAL DETAILS

3.1 Wind tunnel

The RAE 4in × 4in tunnel used for the previous resonance experiments[3] was modified for these tests. The main modification was the provision of two plenum chamber boxes, which could increase d from the datum value ($d = 0.67$) to 2.0 or 4.0. These plenum chamber boxes were bolted directly to the top and bottom of the tunnel shell, as shown in Fig 4. The tunnel shell was provided with four circular access holes to connect the datum plenum chamber to the plenum chamber boxes (see sketch in Fig 5). For comparison with the theory, which refers to a two-dimensional tunnel, large rectangular cut-outs would have been preferred, but this would have weakened the tunnel shell. The access holes leave an adequately strong structure and provide a flush location for the four acoustic tweeters. The lids of the plenum chamber boxes have corresponding access holes.

Another modification was to provide three new pairs of top and bottom liners for the working section, which has closed sidewalls. Two perforated liners with normal holes were made from perforated zinc (meat-safe linings) and Vero-board (a plastic widely used as a base for bread-board circuits). A pair of perforated

liners with 60° inclined holes was available from the previous tests[3]. In addition perforated plates with normal holes used for extensive wind-off tests (Fig 6) were made from hardboard and steel (Table 1). A shallow pair of slotted liners was made to allow comparisons with the original deep slotted liners[3].

For these tests a sidewall static pressure hole (at $x/H = 1.5$) upstream of the usual model position (at $x/H = 2.5$) was used to measure the reference Mach number. This reference pressure was preferred to a plenum chamber pressure because of the wide variations in plenum chamber geometry and the wish to avoid extensive calibrations of the new liners. The reference Mach number was varied from $M = 0.3$ to 0.9. The tunnel total temperature could not be controlled, but varied from about $10^{\circ}C$ to $15^{\circ}C$ during the tests.

3.2 Instrumentation

The acoustic resonances in the working section were excited by four high-frequency one-inch-diameter dome tweeters mounted in either the walls of the plenum chamber or the plenum chamber boxes and driven by an oscillator and a power amplifier.

Each pair of tweeters was wired in phase, but could be switched to operate in phase or in anti-phase with the other pair. All the measurements presented here relate to operation with the top and bottom pairs in anti-phase, because the main interest was to measure the 'odd' resonance frequencies which would be excited by a model oscillating on the tunnel centre line[4]. [Even with the anti-phase switch selected, weak symmetric resonances were excited during the wind-off tests, for no attempt was made to match the acoustic impedances of the tweeters.] During the wind-off tests the tweeters were operated at their maximum rating (8 watts) for several hours without failure. However, during the wind-on tests several tweeters failed after operating for a few minutes at Mach numbers above $M = 0.7$ at ratings of only 4 watts. These failures were attributed to over-heating because of the reduced air density at the higher speeds. Hence the power was reduced to 0.5 watts and no further failures occurred over the subsequent 30 hours of testing.

Seven semi-conductor strain-gauge pressure transducers, having a diaphragm of 3.2 mm diameter, were used to measure the pressure fluctuations across the sidewall of the tunnel at $x/H = 2.0$, $y/H = 0$, ± 0.25, ± 0.44 and ± 0.63 (within the datum plenum chambers). With a pistonphone driven at a single frequency of 50 Hz, the amplifier gains were adjusted to give every transducer the same sensitivity. The frequency response was estimated to be flat from zero up to about 6 kHz.

With the wind on there was initially some difficulty in determining the acoustic resonances against the tunnel noise, particularly at Mach numbers above M = 0.5 and for the deeper cavities. Therefore the amplifier output signals were fed into a tracking filter, locked to the oscillator voltage which excited the tweeters. The tracking filter was a Spectral Dynamics Analyser Type SD 101A, and was used with a 1 Hz bandwidth. This instrument achieved fair repeatability, even at the higher speeds, as indicated by the following table.

Accuracy of frequency measurement (at about 1500 Hz)

Mach number range	Repeatability (Hz)
0	about ±5
0.3 to 0.5	about ±20
0.6 to 0.9	about ±50

Some of this variation might be attributed to variations in the velocity of sound due to changes in the tunnel total temperature, which cannot be controlled.

4 RESULTS

4.1 Duct

When the ventilated liners are removed from the tunnel working section, a duct of height (1 + d)H is formed. The resonance frequencies of this duct at M = 0 must be measured precisely before the frequencies in the presence of the ventilated walls can be correctly predicted.

Fig 5 shows that for d = 0.67 the measured and calculated duct frequencies for the odd modes are almost identical. This is because the acoustic height is almost exactly equal to the geometric height, for the tweeters are flush with the walls of the datum plenum chamber. However, for d = 2.0 and 4.0 the four access holes in the datum tunnel shell significantly increase the effective acoustic height, particularly for the first mode. Thus the measured duct frequencies are appreciably lower than those calculated. The following table shows the acoustic heights which must be used to predict the measured resonance frequencies of the duct correctly.

Geometric height of duct	Acoustic height of duct	
	1st mode	3rd, 5th, etc
0.67	0.67	0.67
2.00	2.87	2.04
4.00	5.11	4.14

The table shows that for the first mode and geometric heights of d = 2 and 4 the access holes in the datum tunnel shell increase the acoustic height by about 1.

The acoustic heights given in the table are used in the calculations without change for all the ventilated liners. These acoustic heights are assumed to be invariant with free-stream Mach number because the mean speed assumed in the plenum chamber is always zero and the assumed variation of plenum-chamber static temperature with Mach number is small. In fact, the true static temperature of air in the plenum chamber is close to the tunnel total temperature and therefore invariant with Mach number (section 2).

4.2 Perforated walls

Fig 6 compares the 1st and 3rd resonance frequencies measured at $M = 0$ for a wide range of perforated walls with results of the new theory. The theory predicts that, as the wall parameter increases, the resonance frequencies fall. Thus for $d = 0.67$, the limit $2kT/H \to \infty$ for the 3rd mode becomes $p = 0.5\pi$, which is the first closed tunnel mode. For the 1st mode the corresponding limit is $p = 0$. The mode shapes change progressively with the changes in frequency. Thus for $d = 0.67$ the 1st mode changes from the 1st closed/closed mode appropriate to a tunnel of height $(1 + d)H$ for $2kT/H = 0$ to a uniform, quiescent mode for $2kT/H = \infty$. Similarly the 3rd mode changes from the 3rd closed/closed mode appropriate to a tunnel of height $(1 + d)H$ for $2kT/H = 0$ to a uniform quiescent mode in both plenum chambers combined with the 1st closed/closed mode appropriate to a tunnel of height H for $2kT/H = \infty$.

For normal holes, theory and experiment are only in excellent agreement for the range of wall parameters currently used in perforated wind tunnels ($0 < 2kT/H < 0.3$). Thus for $d = 0.67$ the resonance frequencies fall significantly as the wall parameter increases, whereas for $d = 2.00$ the variation is smaller; both trends are as predicted by the theory.

For wall parameters higher than 0.3 the measured resonance frequencies are generally higher than predicted. However, in these tests high wall parameters are obtained at the expense of a loss of wall homogeneity, whereas a homogeneous wall is assumed in the theory. Thus for the steel plate the open area ratio was reduced from 40% by taping over streamwise lines of holes forming 'slats' but leaving open three 'slots'. These slots incorporated successively 1, 2 and 3 streamwise rows of holes, which gave open area ratios of 8, 16 and 24%. Despite some lack of homogeneity, the measurements for 24% open area ratio ($2kT/H = 0.30$) are still upon the predicted curves. The hardboard walls have a rectangular grid spacing with only a few large holes and cannot fairly be considered as homogeneous, even with an open area ratio of 4% ($2kT/H = 3.2$). The influence of the lack of

homogeneity becomes less important as the cavities become deeper, as we might have expected from the dispersion allowed by the increased acoustic height. In addition the deeper cavities allow the acoustic excitation to become more uniform.

In contrast to the measurements for normal holes, Fig 6 shows that the measurements for the liners with 60° inclined holes are in excellent agreement with the predictions for both modes and all three plenum depths. This is because the liners with 60° inclined holes are homogeneous, having many small holes. The high wall parameter ($2\,kT/H = 0.86$) is obtained primarily because the open area ratio is only 5% based on the hole area. The effective thickness of the plate to be used in equation (8) is twice the plate thickness because of the 60° inclination of the holes. The general formula suggested for the wall parameter for holes drilled at any angle θ to the normal is

$$2\,kT/H = 2(1 - \sigma)(0.85D + Z \sec \theta)/\sigma H \quad . \tag{20}$$

The wind-on resonance frequency measurements were made either by acoustic excitation from the tweeters or by aerodynamic excitation from the circular cylinders of 10 and 18 mm diameter used in the previous tests[3].

Figs 7, 8 and 9 show the variation of the 1st and 3rd resonance frequencies with Mach number for the three perforated liners. For $d = 0.67$ the acoustic measurements and the theory are in fair agreement. The measured resonance frequencies remain constant up to $M = 0.5$ and then increase to reach a maximum at about $M = 0.7$. For $d = 2.0$ it was more difficult to excite resonances with the tweeters and a comparison between theory and experiment was not generally possible above $M = 0.7$. For the 3rd mode there is some confusion because there are two closely spaced modes in the duct at $M = 0$ (Fig 5) which may be caused by small asymmetries. However, equation (16) has two singularities for $d = 2$, with p near odd multiples of $\pi/2$. With homogeneous perforated walls both modes persist at $M = 0$ and with the wind on. The lower frequency mode generally predominates, and agrees with the theory for $d = 2.04$, as it should.

Figs 7, 8 and 9 also include the resonance frequencies excited by the circular cylinders. Despite careful attempts to excite the 1st mode, this was never detected, possibly because the tunnel was so difficult to control at the low speeds required ($M \doteq 0.2$). However, the 3rd mode could be excited, although the measurements were still difficult at $M = 0.24$. For $d = 0.67$ the cylinder resonance frequencies are appreciably lower than the acoustic measurements, although the difference becomes progressively smaller as the wall parameter

increases from 0.11 to 0.86. We shall see when Fig 13 is discussed in section 4.3 that this difference in frequency is associated with a difference in mode shape. Such a difference is not surprising, given the radical streamwise difference in the two types of excitation and the local Mach number variations about the cylinders. However, for d = 2.0 the third mode resonance frequencies are in excellent agreement with the acoustic measurements. This suggests that the difference between the two types of excitation is much less important for deep cavities. This appears reasonable, for the deeper cavities allow the acoustic excitation to become more uniform.

4.3 Slotted walls

Fig 1 shows measurements at M = 0 of the 1st mode acoustic frequency of a large number of slotted walls. Most of these were cut from cardboard 1 mm thick. The measurements agree with the new theory for all depths of plenum chamber up to wall parameters of about 2 kT/H = 0.5. For wall parameters higher than 0.5 the measured resonance frequencies are higher than predicted. However, most of these high wall parameters relate to a single slot and do not provide the wall homogeneity assumed in the theory. The same trend was noticed previously in the measurements for perforated liners (Fig 6).

Fig 10 presents both the 1st and 3rd modes at M = 0 for the same slotted walls considered in Fig 1. The measurements for the 3rd mode are again in good agreement up to wall parameters of 0.5. Above this wall parameter the measurements are again higher than the theory predicts. This difference becomes progressively smaller as the plenum chamber is deepened, just as for the perforated walls.

Figs 11 and 12 show the variation of the 1st and 3rd resonance frequencies with Mach number for the shallow and deep slotted walls. For d = 0.67 the acoustic modes and the theory are in reasonable agreement. However, for d = 2.0 it was more difficult to excite resonances with the tweeters. At Mach numbers above M = 0.5, the comparison of theory and experiment was less satisfactory. Although for the shallow walls (Fig 11b) there are two closely spaced 3rd modes at M = 0, only one mode can be identified with the wind on. For the deep walls (Fig 12b) only one 3rd mode is found, whether the wind is on or off.

For comparison with the deep hard liners, Fig 12 includes a few acoustic measurements of the resonance frequencies in the slotted working section with the deep laminate liners used in the previous tests[3]. With the deep laminate liners the resonance frequencies are generally a little lower than with the deep hard

liners. The same trend was observed in comparative tests in the RAE 3ft tunnel[12] and was attributed to a small increase in the effective acoustic height of the working section provided by the movement of air into the laminate.

Figs 11 and 12 also include the 3rd and 5th resonance frequencies excited by circular cylinders; the 1st mode could not be excited. The cylinder and acoustic measurements agree for both depths of plenum chamber. The contrast with the differences between cylinder and acoustic measurements observed with the perforated walls for d = 0.67 was so marked that in Fig 13, shapes of the 3rd mode excited by the tweeters and the 10mm diameter cylinder were compared. (The smaller cylinder was selected for the comparison to reduce blockage interference.) Now exact comparisons cannot be expected for two reasons:

(i) there is a large difference in the bandwidths of the pressure fluctuation measurements (only 1 Hz for the acoustic measurements compared to 6.5% of f for the cylinder measurements),

(ii) there is a large difference in signal levels because the resonances excited by the tweeters are about two orders of magnitude smaller than those excited by the cylinders.

To offset these anomalies, both sets of root-mean-square pressure fluctuation measurements, $\bar{p}$, are nondimensionalised by the appropriate reference pressure fluctuation, $\bar{p}_r$, at the point y/H = 0.44 (on the measuring station x/H = 2.0 upstream of the cylinder at x/H = 2.5). Thus, the pressure fluctuations measured at that point by the two radically different methods are forced to coincide and have the value 1. The choice of this point is somewhat arbitrary, but it does not prejudice the comparison.

Fig 13a shows a typical example (for the deep slotted liners at M = 0.31) when the frequencies in Fig 12a were almost identical for d = 0.67. An almost exact match of mode shapes is obtained, which suggests that the reference procedure is reasonable. Fig 13b shows the worst example, for the perforated liners with normal holes at M = 0.32 and a wall parameter of 0.30, when the frequencies in Fig 8a differ by 30%. The mode shapes have the same general character but the acoustic mode shows much larger relative variations across the tunnel. Fig 13c shows an intermediate example (for the perforated wall with 60° inclined holes at M = 0.38) when the frequencies differ by 11%; the acoustic mode still shows the larger relative variation across the tunnel.

Hence we must accept that for d = 0.67, and with perforated walls, the resonances excited by the tweeters and the cylinders differ significantly in

frequency and mode shape. These differences should tentatively be attributed to the three-dimensional nature of the experiment. The tunnel working section length is only four times the tunnel height. The tweeters are disposed along the working section, whereas the cylinder is located at x/H = 2.5 (Fig 5). These streamwise variations in the excitation would become less important with the deeper plenum chambers, and this hypothesis is thus consistent with the experiment.

The dotted curves in Fig 13 show that the root-mean-square pressure fluctuations predicted from equations (A-3) and (A-4) have the same general character as the measurements, and are in good agreement with the cylinder measurements.

4.4 Deep plenum chambers

Ventilated wind tunnels with deep plenum chambers have a multiplicity of closely spaced resonance modes which are difficult to identify at low speeds.

Tests with acoustic excitation for the deep plenum chamber (d = 4) proved even more difficult than for the intermediate plenum chamber (d = 2), particularly at Mach numbers above M = 0.5. Hence only a few typical resonance frequency measurements are presented, for one perforated and one slotted working section (Fig 14).

The acoustic measurements agree with the theory up to M = 0.5. The cylinder excited the 5th mode for the perforated working section and the 5th and 7th modes for the slotted working section. The 3rd mode could not now be excited even by the larger (18mm diameter) cylinder because the resonance frequency had become too low (950 Hz), corresponding with a Mach number of only M = 0.25.

5 DISCUSSION

The measurements presented in section 4 confirm that the depth of the plenum chamber in a small ventilated tunnel has a strong influence on the transverse resonance frequencies up to a Mach number of about M = 0.5. The agreement between the measurements and the predictions is good for both perforated (with normal and 60° inclined holes) and slotted walls. In view of this good agreement, we may infer that the equivalent homogeneous wall boundary conditions in equations (7) and (9) are fairly realistic and might be applied (in conjunction with the appropriate plenum chamber field) to other calculations of dynamic interference which do not involve resonances. However, equation (7) could be unreliable at low frequencies.

Equation (7) assumes that the increase in stream velocity has virtually no influence on the orifice reactance so that the pressure drop lags 90° behind the

outflow velocity. The resonance frequencies predicted under this assumption agree well with the measurements, certainly up to M = 0.5 or U = 170 m/s.

Although as previously noted, Rice predicted that the reactance of normal holes would be unaffected by the stream velocity[10] and this has been confirmed by experiments[13], the measurements of Goldman and Panton[14] suggest that under a turbulent boundary layer the orifice reactance is halved as the stream velocity increases from U = 0 to only U = 30 m/s. Over the same speed range the orifice resistance (*ie* the pressure drop in phase with the outflow velocity) increases by a factor of 10.

These wind-on measurements of Goldman and Panton[14] thus appear inconsistent with the present tests, which cover a much wider speed range.

However, the wind-off measurements of resistance and reactance given in Ref 14 look reasonable, because they agree exactly with the predictions of Hersh and Rogers[9] for thin orifices, despite the large change in plate thickness shown in the table.

Experiment	Frequency	Orifice diameter	Plate thickness
	f (Hz)	D (mm)	Z (mm)
Ref 14	250	5.08	3.2
Ref 9	150	7.0	0.1

Hence, equations (7) and (8) are certainly valid for the perforations used in large transonic tunnels (Table 2) as well as for the small perforations used in the present tests (Table 1).

Accurate estimation of resonance frequencies in large transonic tunnels can be difficult in practice. These tunnels, with height range from 1 m to 5 m, will have low transverse resonance frequencies and a multiplicity of closely spaced modes. The multiple modes may be attributed to small asymmetries, obstructions in the plenum chamber and three-dimensional effects. The three-dimensional effects are always important, even in a nominally two-dimensional working section, because most tunnels have working sections only about three times as long as the height and it is difficult to provide uniform excitation. As an example of these problems, Fig 15 shows two closely spaced fundamental modes (odd modes) excited in the perforated working section (0.91 m × 0.81 m) of the RAE 3ft × 3ft tunnel. (The modes were excited by a single 5 watt loud-speaker mounted in a baffle plate suspended in the middle of the side plenum chamber.) The lowest mode, at 88 Hz, corresponds exactly to the frequency predicted from equation (A-48). The closely spaced mode, at 120 Hz and not predicted by equation (A-48), had a similar mode shape. The large pressure fluctuations in the plenum chamber opposite the loud-speaker, and separated from it by two perforated walls, should be noted. The

amplitudes of both modes were constant across a vertical traverse (Z) at constant values of y , but naturally varied significantly in the streamwise direction. The important point to notice is that the lowest frequency (88 Hz) was correct and that both frequencies were much *lower* than the corresponding closed/closed mode at 183 Hz. Hitherto, guided by Ref 4, wind-tunnel engineers would have anticipated a higher fundamental frequency, of about 1.8 × 183 Hz, although the precise value could not have been predicted for perforated walls. Hence it is recommended that for large transonic tunnels the predictions of the theory for M = 0 according to equation (A-48) should always be compared with a set of measurements with a pair of loud-speakers. Then the symmetric and antisymmetric modes can be carefully separated, as for the present experiments in the small pilot tunnel. The frequencies thus measured should then be used to calculate the effective plenum chamber depth (d) and wall parameter (2 kT/H) to ensure the best match with equation (A-48). These effective values should then be inserted in equations (A-46) and (A-37), for M < 0.618 and M > 0.618 respectively, to predict the wind-on resonance frequencies as a function of Mach number.

The radical change in the solutions which occurs at M = 0.618 has wide implications for the excitation of resonances, both by oscillating models or by flow unsteadiness. For Mach numbers below M = 0.618 the plenum chamber influences the resonance frequencies and is able to dissipate some of the acoustic energy radiated from the working section. Hence we would expect that resonances in ventilated tunnels would be relatively difficult to excite at Mach numbers below M = 0.618. This hypothesis is confirmed by recent experiments with circular cylinders[3,12], which provide a powerful source of excitation up to about M = 0.4. However, for Mach numbers above M = 0.618 the plenum chamber has hardly any influence on the resonance frequencies, and therefore cannot provide much acoustic dissipation. Hence as a general rule we would expect that resonances would be relatively easily excited in ventilated wind tunnels at Mach numbers above M = 0.618, and this is consistent with Varner's observation[15], although he does not consider the influence of the plenum chamber. The pressure fluctuations in the working sections of continuous fan-driven ventilated tunnels generally start to increase rapidly above M = 0.6 (Fig 16). This increase may sometimes correspond to the excitation by the fan of both odd and even resonance modes within the working section. Such resonances could explain the spanwise and vertical variations in pressure fluctuations across the tunnel walls sometimes observed in this speed range.

The flow unsteadiness generally starts to fall above M = 0.8 or 0.85 because the diffuser starts to choke, isolating the working section from the direct influence of the diffuser separations and the fan noise field. Sound-absorbing slats could thus be expected to be particularly useful to reduce flow unsteadiness[3,12] and to attenuate resonances in the Mach number range from M = 0.60 to 0.85.

Now the flow unsteadiness in the plenum chamber of a ventilated tunnel can influence the flow unsteadiness in the working section, even when there are no transverse resonances (see section 5.4.3 in Ref 16) and at supersonic speeds. Hence it would be prudent to make provision for fitting sound-absorbing material in the plenum chambers of all new transonic tunnels, and to measure the pressure fluctuations in the plenum chambers of all transonic tunnels now in use. Following this suggestion, large pressure flunctuations have been measured in the plenum chambers of two blown-down tunnels (the HSA 27in × 27in and the BAC 4ft × 4ft tunnels). These pressure fluctuations correspond to various closed/closed longitudinal organ pipe modes excited by random mixing in the tunnel diffuser, just as in earlier tests in the RAE 3ft tunnel[16]. For the HSA tunnel the plenum chamber unsteadiness has already been reduced by the installation of some sound-absorbing foam. The reduction in plenum chamber pressure fluctuations was accompanied by a reduction of the pressure fluctuations on the centre line and on the walls of the tunnel. For the BAC tunnel a more elaborate configuration of sound-absorbing foam has been installed in the plenum chamber. This has greatly reduced the level of flow unsteadiness in the plenum chamber but comparative measurements are not yet available in the working section.

These resonances excited by the 10 and 18mm diameter cylinders in the present or previous tests[3,12], illustrate interesting examples of a fairly well-known aerodynamic/acoustic interaction. A less well-known interaction of this type occurred during tests of the perforated liners with large normal holes (1.27 mm diameter). When the frequency of the self-induced sound due to the flow over the top and bottom liners coincided with tunnel resonance frequencies, strong resonances were observed in the empty tunnel, independent of the excitation provided by the tweeters. The amplitude of these resonances was intermediate between those excited by the 10 and 18mm diameter cylinders mounted on the tunnel centre line, and those excited by the tweeters in the bottom of the plenum chambers. The Strouhal number based on the hole diameter was very low, only about 0.006 at M = 0.4 and 0.7, possibly because of the outflow induced by the diffuser suction. The normal value[17] without outflow is about 0.20 but may vary with hole diameter[18].

6 CONCLUSIONS

A deficiency in the existing theory to predict resonance frequencies in slotted tunnels has been investigated and attributed to two errors. The first is the neglect of the plenum chamber, the second is the use of an inappropriate boundary condition for the oscillatory flow at the equivalent homogeneous wall. To remedy these errors, an improved theory was developed, which includes the plenum chamber and a better, though still approximate, boundary condition for the equivalent homogeneous wall. The improved boundary condition could be applied in other dynamic interference problems which do not involve resonances but may be unsuitable for low frequencies.

The new theory suggests five main conclusions, which are broadly supported by experiments.

(1) For Mach numbers up to $M = 0.5$ the resonance frequencies depend on the plenum chamber size, as well as upon a wall porosity parameter representing the wall geometry.

(2) For Mach numbers above $M = 0.6$ the resonance frequencies are virtually independent of the plenum chamber size, but still vary with the wall porosity parameter.

(3) The resonance frequencies peak at around $M = 0.70$ in a typical ventilated tunnel.

(4) For all Mach numbers, any flow unsteadiness within the plenum chamber can influence the flow unsteadiness on the tunnel centre line, even when no resonances are excited. Hence the measurement of the pressure fluctuations in the plenum chambers of all ventilated tunnels is strongly recommended.

(5) If large plenum chamber pressure fluctuations are discovered, they may often be attenuated by acoustic treatment, with resulting improvements in the working section.

These conclusions are of particular interest to engineers who use ventilated wind tunnels for any kind of dynamic test, such as the measurement of flutter speeds, unsteady control-surface characteristics, rigid-body aerodynamic derivatives or the severity of buffeting. If the test frequency happens to coincide with a tunnel resonance frequency the results should always be evaluated with caution.

Appendix

CALCULATION OF THE RESONANCE FREQUENCIES OF VENTILATED TUNNELS

The two-dimensional ventilated tunnel is idealised as shown in Fig 2. The mean velocity, U , is uniform in the free-stream flow and zero in the plenum chamber. The mean static pressure and density are assumed to be uniform across the working section and plenum chamber. Solutions of the appropriate disturbance potential equations in the free-stream flow (ϕ) and the plenum chamber flow (ψ) are matched along the boundaries of the working section (at $z = \pm H/2$). On this thin wall discontinuities in streamwise velocity are allowed. However, on both sides of the wall the normal velocity must be identical to satisfy the equation of continuity of mass flow, so that:

$$\phi_z = \psi_z \quad . \tag{A-1}$$

At the outer boundaries of the plenum chamber {at $z = \pm H(1 + d)/2$} we must apply the condition of no normal velocity.

$$\psi_z = 0 \quad . \tag{A-2}$$

Following Acum (equation (4.4), Chapter IV of Ref 5) we may write the linearised expression for the pressure in the free stream as:

$$p - p_\infty = -\rho[U\phi_x + \phi_t] \quad . \tag{A-3}$$

Similarly the plenum chamber pressure is:

$$p - p_\infty = -\rho[\psi_t] \quad . \tag{A-4}$$

Hence the pressure drop across the homogeneous walls at $z = \pm H/2$ is:

$$p_w = -\rho[U\phi_x + \phi_t - \psi_t] \quad . \tag{A-5}$$

Different expressions for equation (A-5) are now developed for perforated and slotted walls, before we find the appropriate solutions of the disturbance potential equations.

Perforated walls

For small oscillatory flows through a single orifice normal to the surface into air at rest, we know from both theory and experiment[9] that the oscillatory velocity lags nearly 90^{o} behind the applied oscillatory pressure for high frequencies. For a single orifice of diameter D and depth Z we may write

$$p_w = i\rho\omega(0.85D + Z)V_0 \quad , \tag{A-6}$$

where V_0 = oscillatory flow through the orifice. We will assume that equation (A-6) applies when there is flow across the orifice. For a number of identical small orifices in a plate of open area ratio, σ, we may write an equivalent homogeneous boundary condition on the normal velocities as

$$V_n = \sigma V_0 \quad . \tag{A-7}$$

Hence, if we assume that there are no interactions between the flow around neighbouring perforations, we find from equations (A-6) and (A-7) that

$$p_w = i\rho\omega(0.85D + Z)V_n/\sigma \quad . \tag{A-8}$$

More generally we may write

$$p_w = i\rho\omega T k V_n \quad , \tag{A-9}$$

where $$T = (0.85D + Z) = \text{effective hole diameter} \quad , \tag{A-10}$$

and k is a dimensionless function of the open area ratio σ, which should be found from experiment. A simple empirical function for k which would satisfy the correct limits for $\sigma = 0$ and $\sigma = 1$ is

$$k = (1 - \sigma)/\sigma \quad , \tag{A-11}$$

and this should suffice to indicate the variation with open area ratio in the range normally utilized (say $\sigma < 0.25$).

Thus from equations (A-5) and (A-9) we find for $z = \pm H/2$

$$\phi_x + (\phi_t - \psi_t)/U \pm (ik\omega T/U)\phi_z = 0 \quad . \tag{A-12}$$

Slotted walls

We assume that the expression for p_w given in equation (A-5) may be equated with the pressure drop required to cause the streamline curvature ϕ_{xz}/U, in accord with the homogeneous boundary condition developed previously for steady flow in equation (1). Hence we find that for $z = \pm H/2$,

$$\phi_x + (\phi_t - \psi_t)/U \pm (FH/2)\phi_{xz} = 0 \quad . \tag{A-13}$$

Solutions of equations for the velocity potential

For the mainstream flow we follow Acum and write

$$(1 - M^2)\phi_{xx} + \phi_{zz} - 2\phi_{xt}M^2/U - M^2\phi_{tt}/U^2 = 0 \quad . \tag{A-14}$$

We choose

$$\phi = A \sin \lambda z e^{i\alpha x} e^{i\omega t} \quad , \tag{A-15}$$

thus ensuring that at a resonance condition, excited by a model oscillating on the tunnel centre line,

$$\phi_z \neq 0 \quad . \tag{A-16}$$

The wind-tunnel configuration is symmetric and therefore we consider only anti-symmetric solutions of ϕ and ψ, valid for $0 < z < H(1 + d)/2$.

From equations (A-14), (A-15) and Acum's equation (7) we find that the eigenvalues, λ, satisfy

$$\alpha = M^2\omega/U\beta^2 = M^2\beta U\lambda/U\beta^2 M = M\lambda/\beta \quad , \tag{A-17}$$

where

$$\beta = (1 - M^2)^{\frac{1}{2}} \quad . \tag{A-18}$$

Now for the plenum flow,

$$M = U = 0 \quad ,$$

and the disturbance potential is given by the acoustic wave equation (see J.W. Miles, Ref 19, section 2.5). Thus

$$\psi_{xx} + \psi_{zz} = \psi_{tt}/a_0^2 \tag{A-19}$$

where a_0 = velocity of sound in the plenum chamber.
The acoustic wave equation must be used because the limit $M \to 0$ in equation (A-14) does not necessarily imply incompressible flow when $U \to 0$.

Solutions of equation (A-19) compatible with equation (A-15) must be of the form

$$\psi = g(z)e^{i\alpha x}e^{i\omega t} \quad , \tag{A-20}$$

so that from equations (A-19) and (A-20)

$$g_{zz} - \left(\alpha^2 - \omega^2/a_0^2\right)g = 0 \quad . \tag{A-21}$$

If we write

$$E^2 = \alpha^2 - \omega^2/a_0^2 \quad , \tag{A-22}$$

equation (A-21) becomes

$$g_{zz} - E^2 g = 0 \quad , \tag{A-23}$$

and the character of the solution of the plenum chamber flow will be determined by the sign of E^2 , which is influenced by the free-stream Mach number, M , and the speed of sound in the plenum chamber, a_0 . By our assumption of constant pressure and density across the tunnel, the static temperature of the air in the free stream and the plenum chamber are identical. Hence

$$a_0 = U/M \quad . \tag{A-24}$$

Then from equations (A-17), (A-22) and (A-24),

$$E^2 = M^2\lambda^2/\beta^2 - \beta^2\lambda^2 \quad ,$$

or

$$Q = E/\lambda = \left[M^2/(1 - M^2) - (1 - M^2)\right]^{\frac{1}{2}} . \tag{A-25}$$

The form of solution to equation (A-23) will depend on whether Q is real or complex.

First we treat the special case $Q = 0$, when from equation (A-25)

$$M = 0.618 \quad . \tag{A-26}$$

Then we deal separately with the speed ranges $M > 0.618$ (Q real) and $M < 0.618$ (Q pure imaginary).

Before doing this, it is convenient to note that the boundary conditions on the ventilated walls at $z = \pm H/2$ may now be specified, using equations (A-15), (A-17) and (A-20).

For perforated walls, we find from equation (A-12), writing

$$p = \lambda H/2 \quad . \tag{A-27}$$

$$\boxed{A \sin p - \beta^2 g(H/2) + (2A\beta^2 kT/H)p \cos p = 0} \quad . \tag{A-28}$$

For slotted walls, we find from equation (A-13)

$$\boxed{A \sin p - \beta^2 g(H/2) + (M^2 AF)p \cos p = 0} \quad . \tag{A-29}$$

$\underline{M = 0.618}$ $(Q = 0)$

When $Q = 0$, equation (A-23) becomes $g_{zz} = 0$, which has the simple solution (for $H/2 \leqslant z \leqslant H(1 + d)/2$) ,

$$g = G_1 + G_2 z \quad ; \tag{A-30}$$

where G_1 and G_2 are constants. Now on the outer wall of the plenum chamber we must have from equation (A-2)

$$g_z = 0 \quad ,$$

so that from equation (A-30)

$$G_2 = 0 \quad , \tag{A-31}$$

and there is no normal velocity across the plenum chamber. For the ventilated, inner wall of the plenum chamber we must also satisfy equation (A-1) so that from equation (A-15)

$$A\lambda \cos(\lambda H/2) = A\lambda \cos p \equiv 0 \quad . \tag{A-32}$$

Hence $p = \pi/2$, $3\pi/2$ etc, the same values as found previously for the closed tunnel by Acum. It is surprising that the eigenvalues at this speed should be independent of the wall geometry or the size of the plenum chamber. In particular,

at this speed the resonance frequencies of perforated and slotted tunnels are identical and equations (A-28) and (A-29) assume the same degenerate form independent of the wall parameters:

$$A \sin p - \beta^2 g(H/2) = 0 \quad , \quad \text{or} \quad G_1 = (A \sin p)/\beta^2 \quad . \tag{A-33}$$

High speeds ($M > 0.618$, Q real)

From equation (A-2) we have $g_z \equiv 0$ when $z = H(1 + d)/2$ so that from equation (A-23)

$$g = B \cosh [\, E\{H(1 + d)/2 - z\}] \quad . \tag{A-34}$$

Different solutions are now obtained by satisfying the boundary condition at the perforated or slotted walls.

At both perforated and slotted walls, we find from equation (A-1) and (A-34)

$$A\lambda \cos p + BE \sinh (EdH/2) = 0 \quad . \tag{A-35}$$

At a *perforated* wall we find from equations (A-34) and (A-28)

$$A \sin p - B\beta^2 \cosh (EdH/2) + A(2\beta^2 kT/H)p \cos p = 0 \quad . \tag{A-36}$$

Hence we find from equations (A-25), (A-35) and (A-36)

$$\boxed{\tan p + (\beta^2/Q) \coth (Qdp) + (2\beta^2 kT/H)p = 0} \quad . \tag{A-37}$$

The limiting solutions of equation (A-37) are of interest. When the perforated wall becomes fully closed

$$k \to \infty$$

so that

$$\tan p = -\infty \quad . \tag{A-38}$$

Hence, $p = \pi/2$, $3\pi/2$ etc the odd eigenvalues appropriate to the closed tunnel. When the perforated wall is removed we have an open jet surrounded by a plenum chamber and

$$k \to 0$$

so that

$$\tan p \tanh (Qdp) = - \beta^2/Q \quad . \tag{A-39}$$

For an infinitely small plenum chamber, $d \to 0$ and equation (A-39) becomes

$$\tan p = - \infty \tag{A-38}$$

again giving the equation appropriate to a closed tunnel, as required by the boundary condition on the outer wall of the plenum chamber. In contrast, for an open jet with an infinitely large plenum chamber we find that

$$\tan p = - \beta^2/Q \quad . \tag{A-40}$$

At a *slotted* wall we find from equations (A-34) and (A-29)

$$\boxed{\tan p + (\beta^2/Q) \coth (Qdp) + M^2 Fp = 0} \quad . \tag{A-41}$$

Equation (A-41) has identical limiting solutions to equation (A-37).

Low speeds ($M < 0.618$, Q pure imaginary)

It is convenient to write $E^2 = - J^2$
where J is a positive real number.
Equation (A-23) then becomes:

$$g_{zz} + J^2 g = 0 \quad ,$$

which has the solution

$$g = L \cos \left[J\{H(1 + d)/2 - z\}\right] \quad , \tag{A-42}$$

to satisfy the boundary condition on the outer wall of the plenum chamber (A-2).

At both perforated and slotted walls we find from equations (A-42) and (A-1)

$$A\lambda \cos p - LJ \sin (JdH/2) = 0 \quad . \tag{A-43}$$

At a *perforated* wall we find from equations (A-42) and (A-28)

$$A \sin p - L\beta^2 \cos (JdH/2) + (2A\beta^2 kT/H)p \cos p = 0 \quad . \tag{A-44}$$

For brevity we may write

$$J/\lambda = \left[(1 - M^2) - M^2/(1 - M^2)\right]^{\frac{1}{2}} = R \ , \qquad \text{(A-45)}$$

so that equations (A-43) and (A-44) give

$$\boxed{\tan p - (\beta^2/R) \cot (Rdp) + (2\beta^2 kT/H)p = 0} \ . \qquad \text{(A-46)}$$

The limiting solutions of equation (A-46) are of interest. When the wall is fully closed $k \to \infty$ so that equation (A-46) reduces to equation (A-38). When the perforated wall is removed we have an open jet with $k = 0$ so that equation (A-46) becomes

$$\tan p \tan (Rdp) = \beta^2/R \ . \qquad \text{(A-47)}$$

With an infinitely small plenum chamber round the open jet $d \to 0$ so that equation (A-47) reduces to equation (A-38), as required by the boundary condition on the outer wall of the plenum chamber.

When the speed of the tunnel is reduced to zero, $R = 1$ and equation (A-46) becomes

$$\boxed{\tan p - \cot (dp) + (2kT/H)p = 0} \ . \qquad \text{(A-48)}$$

When the perforated wall is removed, $k = 0$ and we find that the solution of equation (A-48) is then $p = n\pi/2(1 + d)$,
where n is an odd integer which we recognise as the odd eigenvalues for the closed organ pipe of height $(1 + d)H$, as required by the boundary conditions on the outer wall of the plenum chamber.

At a *slotted* wall we find from equations (A-42) and (A-29)

$$A \sin p - L\beta^2 \cos (JdH/2) + M^2 AFp \cos p = 0 \ . \qquad \text{(A-49)}$$

Hence from equations (A-43) and (A-49)

$$\boxed{\tan p - (\beta^2/R) \cot (Rdp) + M^2 Fp = 0} \ . \qquad \text{(A-50)}$$

Equation (A-50) has the same limiting solutions for a closed tunnel ($F \to \infty$) or an open tunnel ($F = 0$) as equation (A-46). However, when the tunnel speed is reduced to zero equation (A-50) gives a different limiting solution:

$$\tan p \tan (dp) = 1 \quad . \tag{A-51}$$

We find by inspection that this has the solution

$$p = n\pi/2(1 + d) \qquad (n = 1, 3, 5 \text{ etc})$$

independent of the value of F ($F = \infty$ being excluded).

The previous solutions all relate to resonance modes excited by a model oscillating on the tunnel centre line, and therefore subject to equation (A-16). However, in an empty, ventilated tunnel additional resonance modes might be excited by flow unsteadiness. These modes may be found by replacing the free-stream velocity potential (A-15) by

$$\phi = A \cos \lambda z e^{i\alpha x} e^{i\omega t} \quad . \tag{A-52}$$

With this potential the boundary conditions on the homogeneous walls are altered. For perforated walls equation (A-28) is replaced by:

$$\boxed{A \cos p - \beta^2 h(H/2) - (2A\beta^2 kT/H)p \sin p = 0} \quad . \tag{A-53}$$

For slotted walls equation (A-29) is replaced by:

$$\boxed{A \cos p - \beta^2 g(H/2) - (AM^2 F)p \sin p = 0} \quad . \tag{A-54}$$

Then for high speed flows equation (A-37) for perforated walls is replaced by

$$\boxed{\cot p - (\beta^2/Q) \coth (Qdp) - (2\beta^2 kT/H)p = 0} \quad . \tag{A-55}$$

For slotted walls equation (A-41) is replaced by

$$\boxed{\cot p - (\beta^2/Q) \coth (Qdp) - (M^2 F)p = 0} \quad , \tag{A-56}$$

when either k or $F \to \infty$, or $d \to 0$ equations (A-55) and (A-56) become:

$$\cot p = \infty \tag{A-57}$$

so that $p = \pi$, 2π, etc the even eigenvalues for a closed tunnel.
For low speed flows equation (A-46) for a perforated wall is replaced by:

$$\boxed{\cot p + (\beta^2/R) \cot(Rdp) - (2\beta^2 kT/H)p = 0} \quad . \tag{A-58}$$

When the wall is fully closed $k \to \infty$ and equation (A-58) reduces to equation (A-57). When the free-stream flow is reduced to zero, $R \to 1$ and equation (A-58) becomes:

$$\cot p + \cot (dp) - (2kT/H)p = 0 \quad . \tag{A-59}$$

When the perforated wall is removed $k \to 0$ and equation (A-59) becomes:

$$\cot p + \cot (dp) = 0 \quad . \tag{A-60}$$

This has the solution

$$p = m\pi/(1 + d) \quad , \tag{A-61}$$

where m is any integer which we recognise as the even eigenvalues of a closed organ pipe of height $(1 + d)H$.

Similarly equation (A-50) for a slotted wall is replaced by:

$$\boxed{\cot p + (\beta^2/R) \cot (Rdp) - M^2Fp = 0} \quad . \tag{A-62}$$

Equation (A-62) has the same limiting solutions for a closed tunnel ($F = \infty$) or an open tunnel ($F = 0$) as equation (A-58). However, when the free-stream flow is reduced to zero $R \to 1$ and equation (A-62) reduces to equation (A-60) for all finite values of F .

It is reasonable that the characteristics of the perforated wall should influence the tunnel resonance at zero stream velocity through equations (A-48) and (A-59). However, the contrasting result that the corresponding resonance condition in a slotted tunnel should be independent of slot geometry through equations (A-51) and (A-60) is one that challenges intuition. It casts some doubt on the general validity of the boundary condition (A-13) for unsteady flow at a slotted wall.

Table 1

DETAILS OF LINERS FOR SMALL TUNNEL (H = 102 mm)

Perforated (see Fig 6)	Open Area (%)	Hole diameter (mm)	Thickness (mm)	Grid	2kT/H
Normal holes:					
'Vero-board'	13	1.05	1.5	Rectangular	0.30
Zinc	26	1.27	0.9	Staggered	0.11
Hardboard	2.4 and 4.0	4.5	3.5	Rectangular	5.2 and 3.2
Steel	8 to 40	4.5	1.0	Staggered	1.1 to 0.15
60^{o} inclined:					
Perspex	5	0.79	0.79	Staggered	0.86

Slotted (see Fig 1)	Open area (%)	Slot width (mm)	Depth (mm)	2kT/H
1 slot	12 to 100	12 to 102	1	1.63 to 0
3 slots	12, 24, 36	4, 8, 12	1	0.64 to 0.40
5 slots	10 and 20	2, 4	1	0.49 and 0.35
	18	3.4	3	0.53
	18	3.4	16	1.72

Table 2

REFERENCE VALUES FOR LARGE PERFORATED TUNNELS IN UK

Perforation	Open area (%)	Hole diameter (mm)	Depth (mm)	Grid	2kT/H
Normal holes:					
HS 27 × 27 in	22	9.5	6.4	Staggered	0.15
BAC 4 × 4 ft	19	15.8	9.5	Staggered	0.16
ARA 9 × 8 ft	22.5	12.7	48	Staggered	0.04
60^{o} inclined:					
RAE 3 × 3 ft	6	9.5	9.5	Staggered	0.95

LIST OF SYMBOLS

a	slot spacing
a_t	velocity of sound in settling chamber at total temperature
b	slot width
d	ratio of total plenum chamber depth to tunnel height
D	cylinder or hole diameter
F	wall factor for slotted tunnels in equation (1)
f	frequency (Hz)
H	tunnel height
$k = (1 - \sigma)/\sigma$	empirical porosity factor
M	Mach number
n	resonance mode number
p	eigenvalues of solutions for resonance frequencies
$\bar{p}$	rms pressure fluctuation
$\bar{p}_r$	rms reference pressure fluctuation
R	Reynolds number per unit length
S^*	Strouhal number - equation (17)
$T = 0.8D + Z$	equivalent hole diameter
t	time
U	free stream velocity
x,y,z	coordinates centred on tunnel centre line (Fig 2)
Z	plate thickness
σ	open area ratio
ϕ	velocity potential of free stream flow
ϕ_1,ϕ_2	angles of incident and refracted waves (Fig 3)
ψ	velocity potential of plenum chamber flow
ω	circular frequency = $2\pi f$ rad/s

REFERENCES

No.	Author	Title, etc
1	H.L. Runyan D.S. Woolston A.G. Rainey	Theoretical and experimental investigation of the effect of tunnel walls on the forces acting on an oscillating airfoil in two-dimensional compressible flow. NACA Report 1262 (1956)
2	J.P. Hartzuiker P.G. Pugh W. Lorenz-Meyer G.E. Fasso	On the flow quality necessary for the large European high Reynolds number transonic wind tunnel LEHRT. AGARD Report R644, March 1976
3	D.G. Mabey	The use of sound absorbing walls to reduce dynamic interference in wind tunnels. ARC R & M No.3831 (1976)
4	W.E. Acum	A simplified approach to the phenomenon of wind tunnel resonance. ARC R & M No.3371 (1962)
5	W.E. Acum	Subsonic wind tunnel wall corrections - Chapter IV. Interference effects in unsteady experiments. AGARDograph 109 (1966)
6	D.D. Davis D. Moore	Analytical study of blockage and lift interference corrections to slotted tunnels obtained by the substitution of an equivalent homogeneous boundary for the discrete slots. NACA RM L53E07b (1953)
7	H. Lamb	Hydrodynamics. Chapter X, Article 306, Cambridge University Press (1932)
8	D.L. Smith L.L. Shaw	Prediction of the pressure oscillations in cavities exposed to aerodynamic flow. AFFDL-TR-75-34, October 1975
9	A.S. Hersh T. Rogers	Fluid mechanical model of the acoustic impedance of small orifices. NASA CR-2682, May 1976
10	E.J. Rice	A theoretical study of the acoustic impedance of orifices in the presence of a steady grazing flow. NASA TMX 71903, April 1976

REFERENCES (concluded)

No.	Author	Title, etc
11	P.M. Morse K.U. Ingard	Theoretical acoustics, Chapter 11 - Acoustics in moving media. McGraw Hill (1968)
12	D.G. Mabey	The reduction of dynamic interference by sound-absorbing walls in the RAE 3ft tunnel. ARC R & M No.3837 (1977)
13	A.S. Hersh B. Walker	Effects of grazing flow on the steady state resistance and acoustic impedance of thin porous liners. NASA CR-2951, January 1978
14	A.L. Goldman R.L. Panton	Measurements of the acoustic impedance of an orifice under a turbulent boundary layer. J. Acoust, Soc. Am., Vol 60, No.6, pp 1397-1404 (1976)
15	M.O. Varner	Noise generation in transonic wind tunnels. AEDC TR 74-126 (1975)
16	D.G. Mabey	Some remarks on the design of transonic tunnels with low levels of flow unsteadiness. NASA CR-2722, August 1976
17	A.B. Bauer R.C. Chapkis	Noise generated by boundary layer interaction with perforated acoustic liners. AIAA Paper 76-41 (1976)
18	C.Y. Tsui	Experimental observations of self induced sound generation due to flow over perforated liners in a duct. ISVR Technical Report No.70 (1974)
19	J.W. Miles	The potential theory of unsteady supersonic flow. Cambridge University Press (1959)

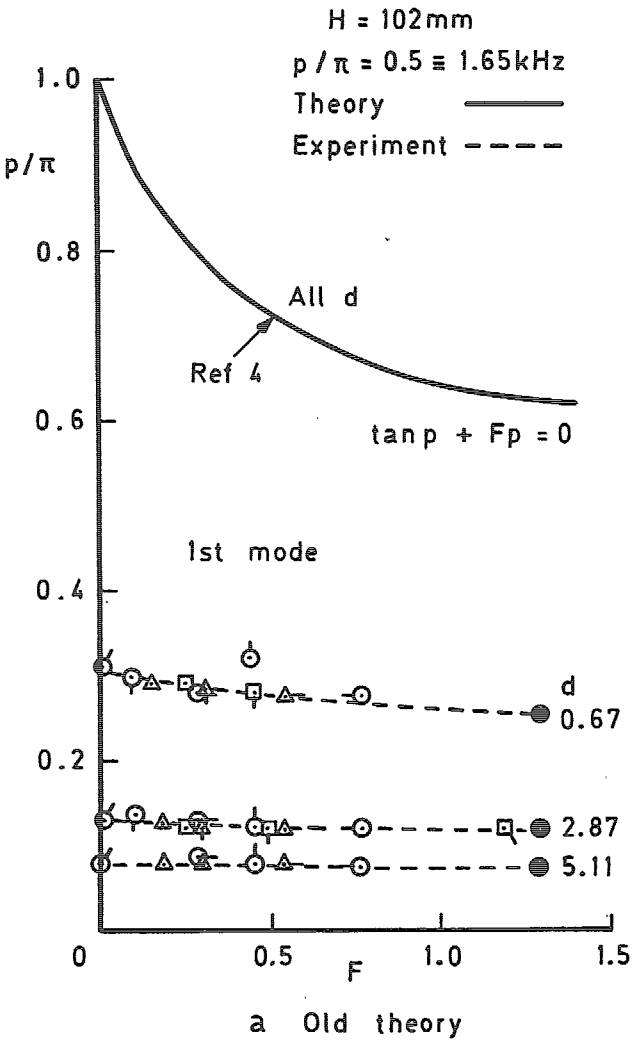

a Old theory

Slots	Open area (%)	F	2kT/H	Depth (mm)
1	12	1.28	1.63	1
	24	0.76	1.35	
	36	0.46	1.14	
	50	0.28	0.87	
	75	0.09	0.43	
	100	0	0	
3	12	0.54	0.64	
	24	0.29	0.49	
	36	0.18	0.40	
5	10	0.46	0.49	
	20	0.25	0.35	
	18	0.55	0.53	3
	18	2.04	1.72	16

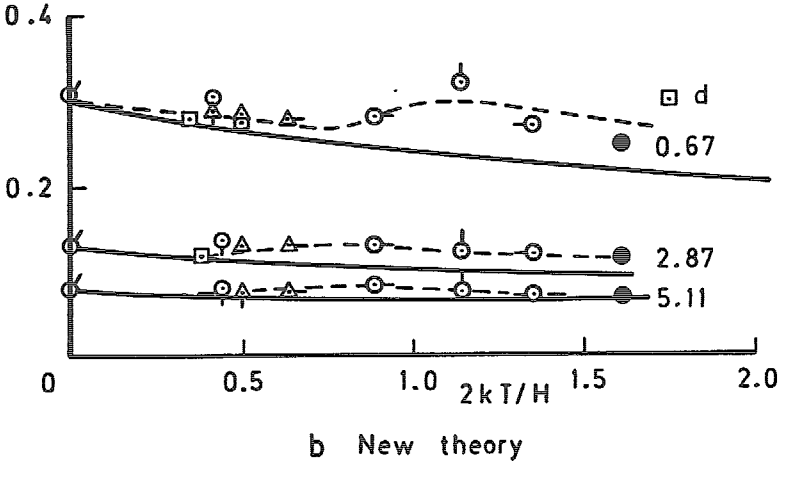

b New theory

Fig 1a&b Slotted tunnels — resonance frequencies at M = 0

Fig 1a&b

Fig 2

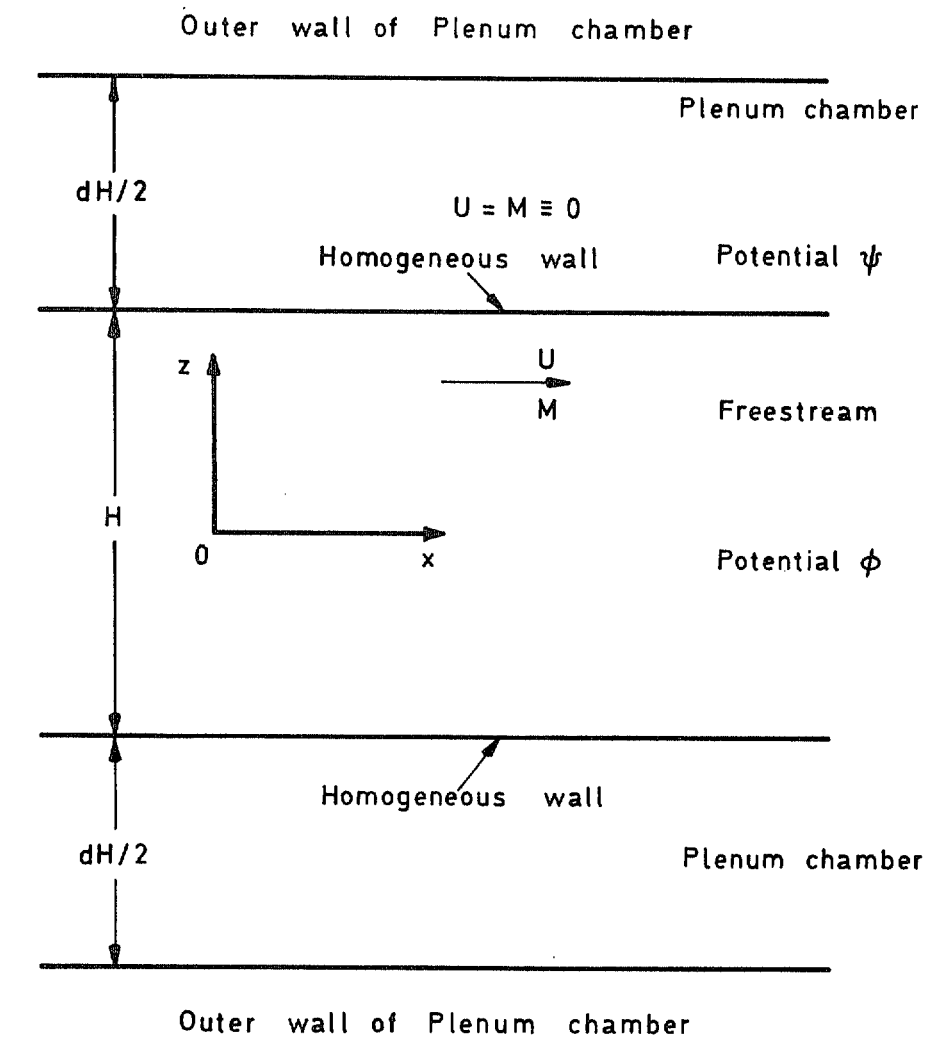

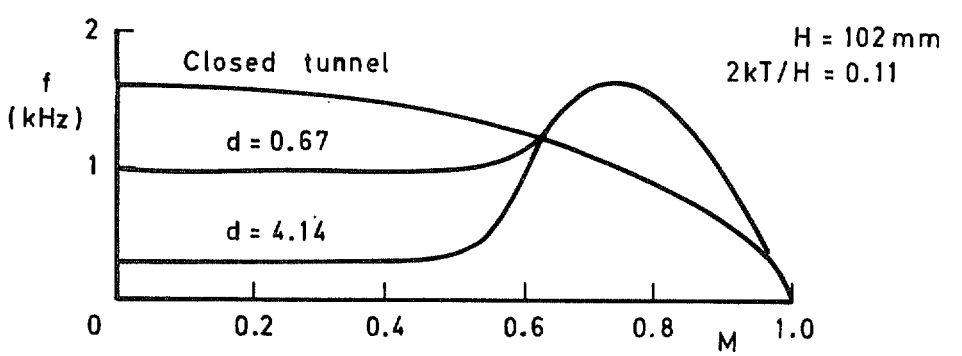

Fig 2 Notation for calculation of resonance frequencies and typical dependence on Mach number

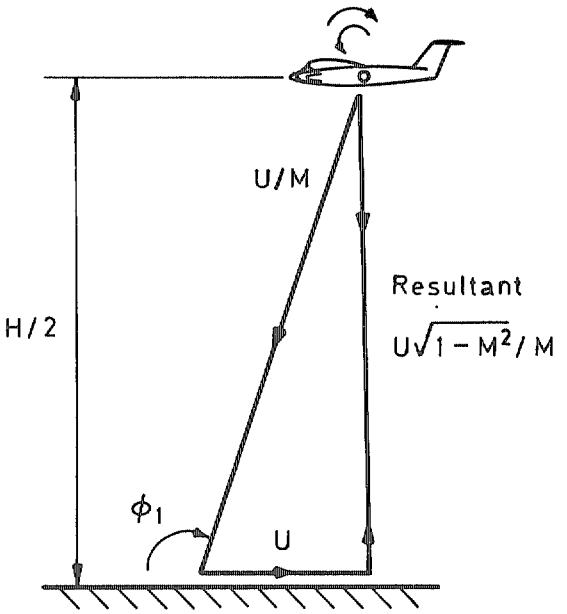

a Closed – reflection

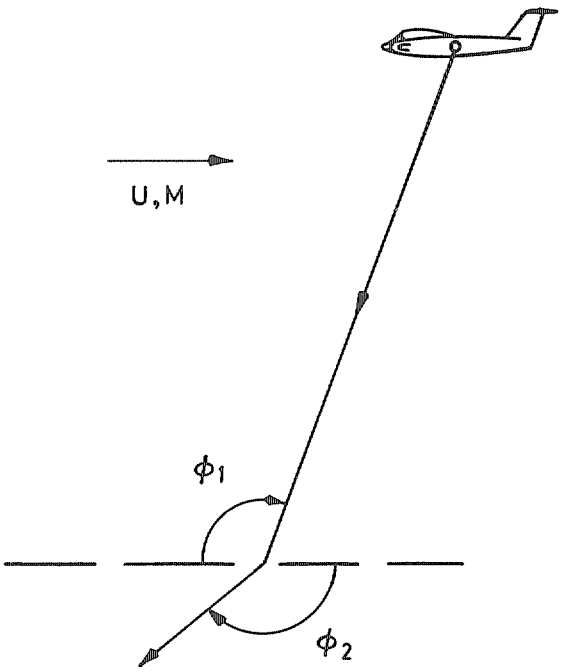

b Open – refraction

$$\cos \phi_2 = \frac{\cos \phi_1}{(1 + M \cos \phi_1)}$$

Fig 3a&b Acoustic ray theory

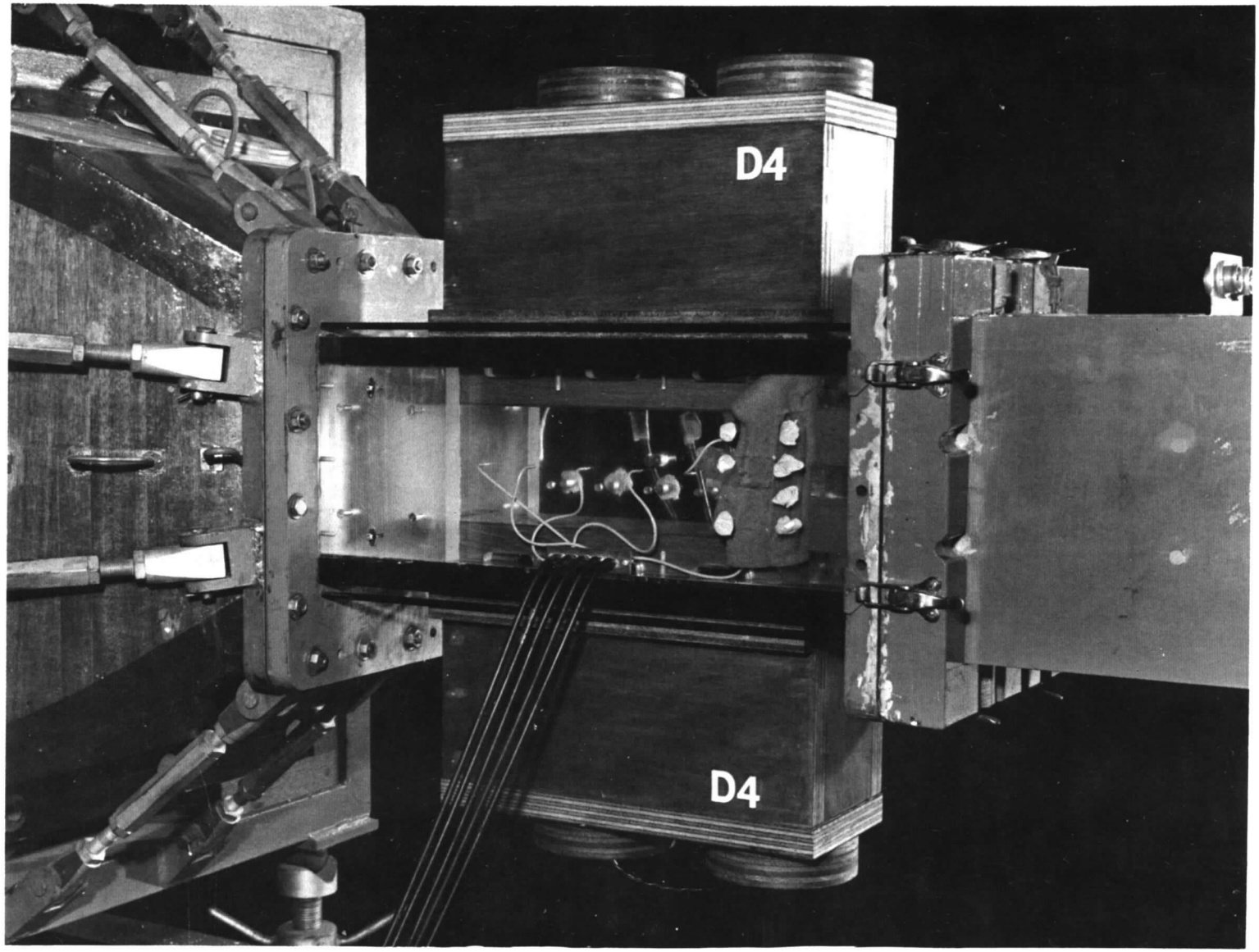

Fig 4 Modified RAE 4in x 4in tunnel (d = 4)

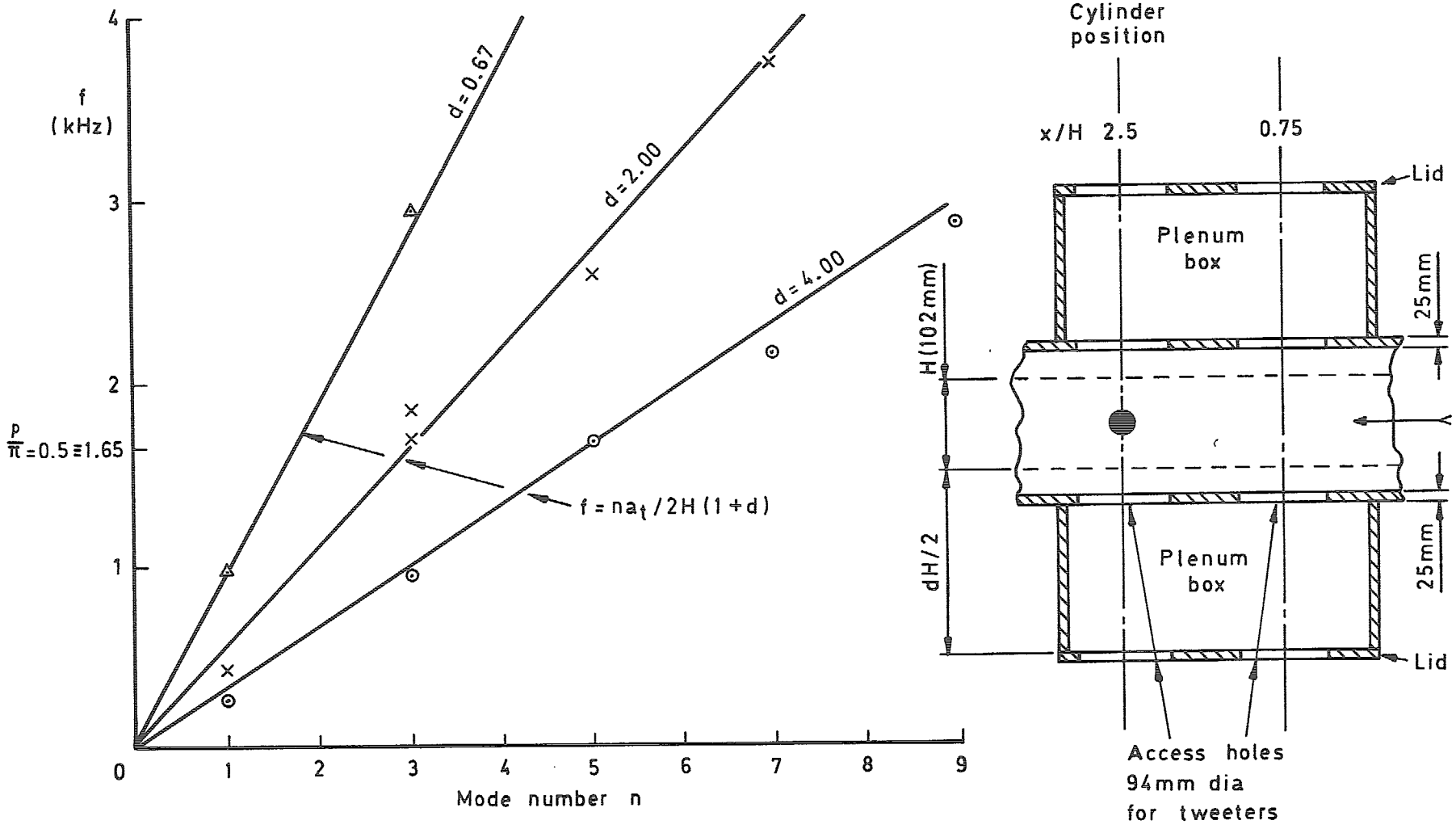

Fig 5 Duct resonance frequencies — M = 0 (antiphase mode)

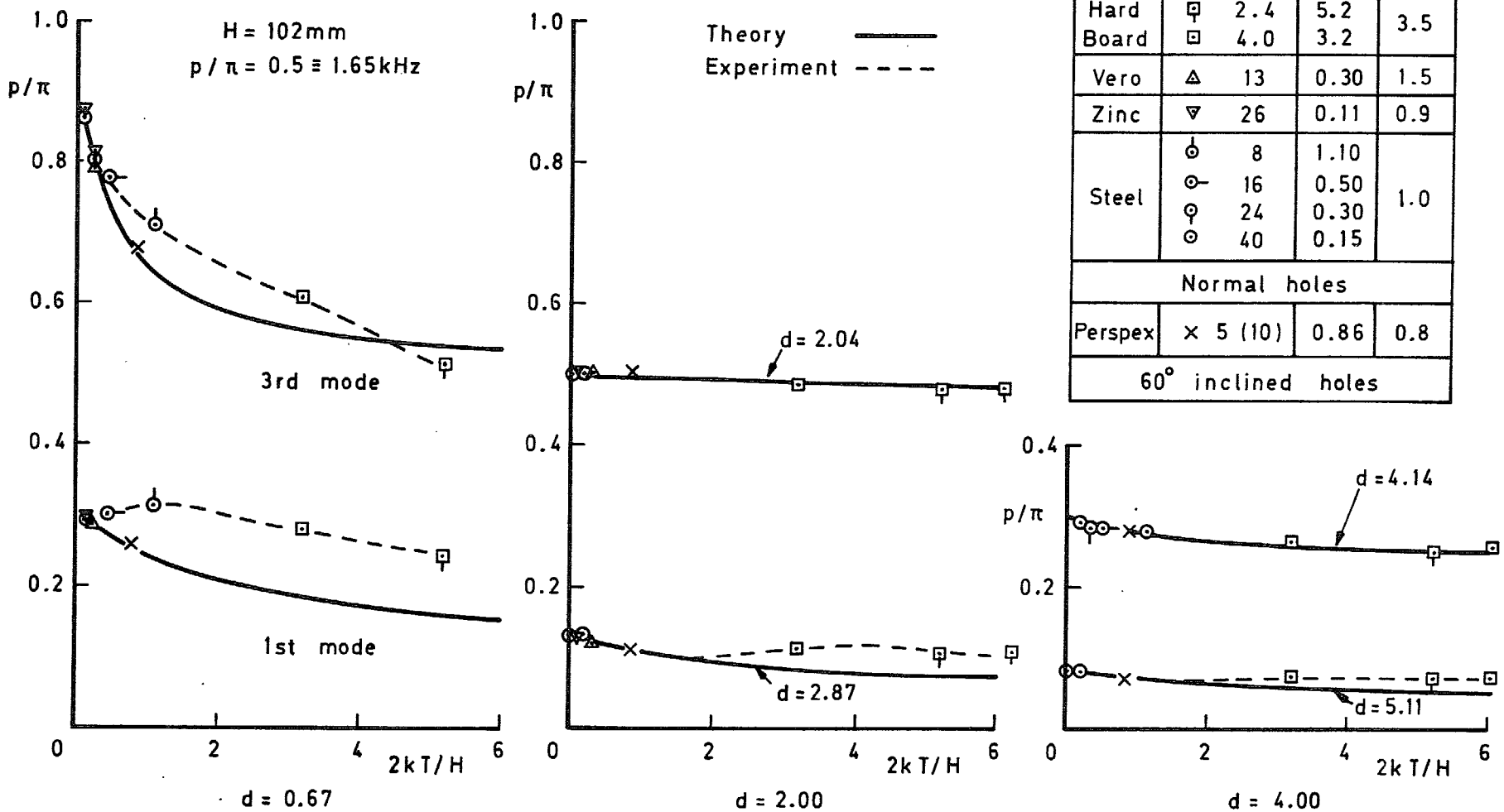

Plate	Open area %	2k T/H	Depth (mm)
Hard Board	2.4	5.2	3.5
	4.0	3.2	
Vero	13	0.30	1.5
Zinc	26	0.11	0.9
Steel	8	1.10	1.0
	16	0.50	
	24	0.30	
	40	0.15	
Normal holes			
Perspex	× 5 (10)	0.86	0.8
60° inclined holes			

Fig 6 Perforated walls – resonance frequencies at M = 0

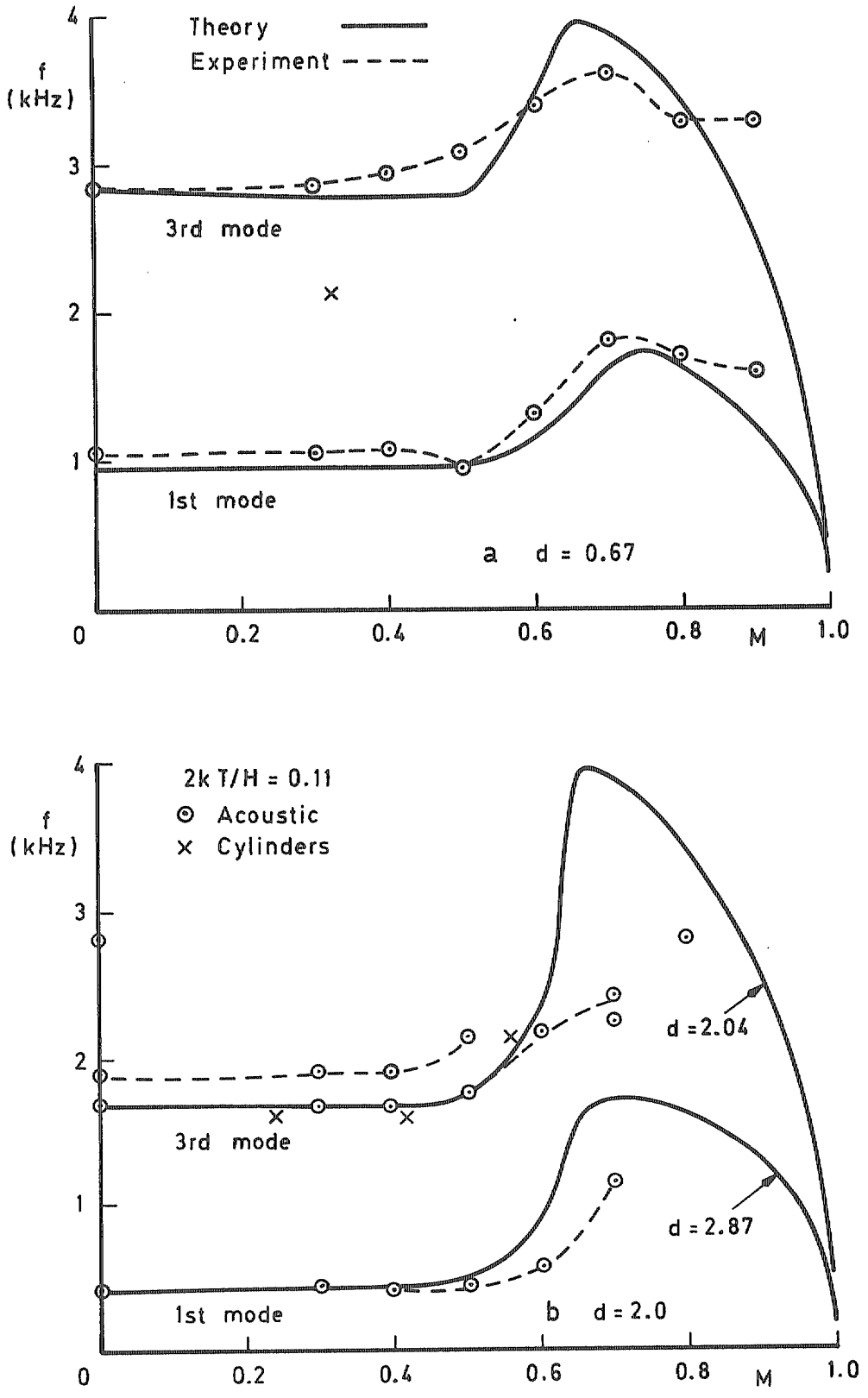

Fig 7 Perforated walls (26% open) — resonance frequencies v Mach number

Fig 8

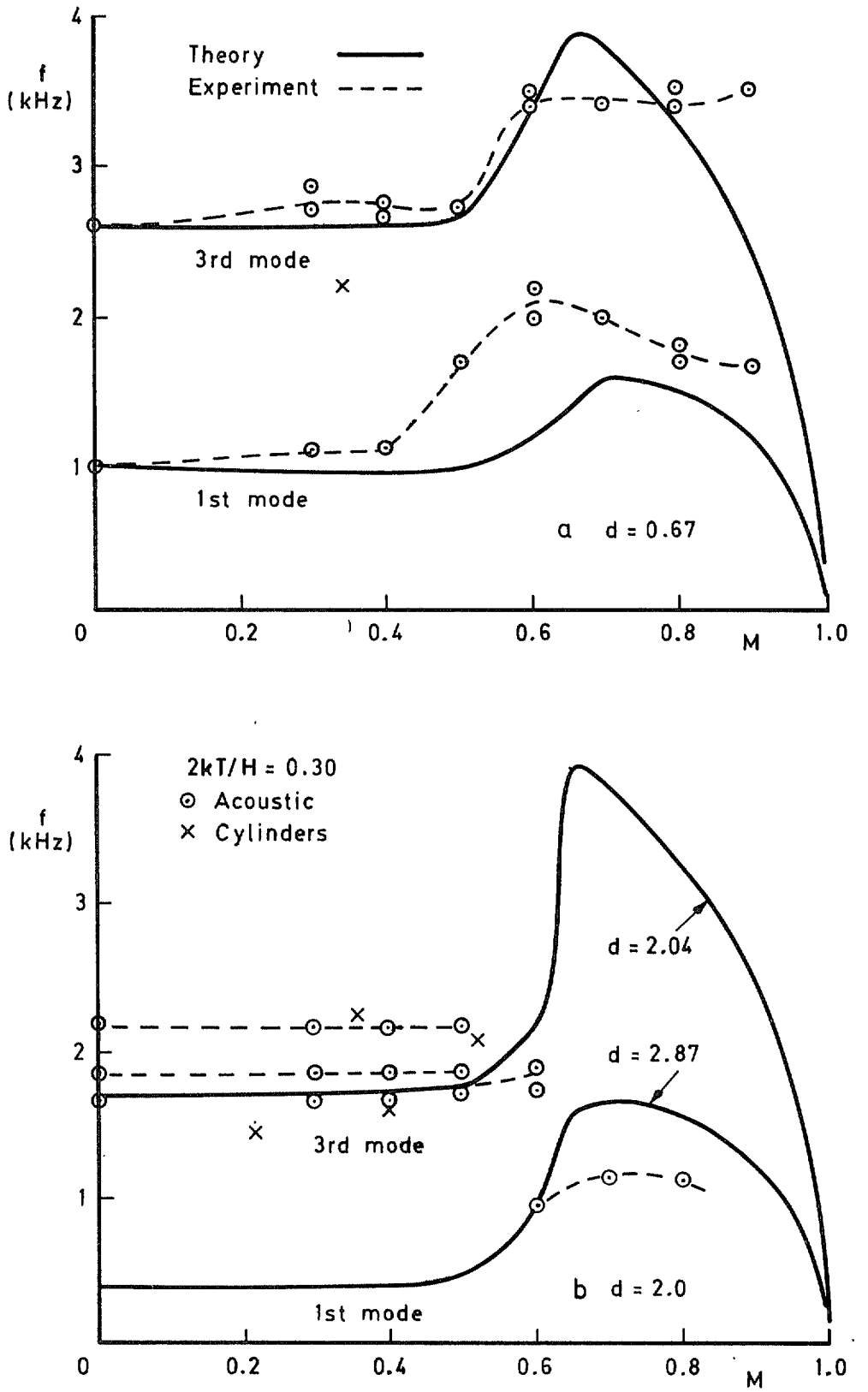

Fig 8 Perforated walls (13% open) -- resonance frequencies v Mach number

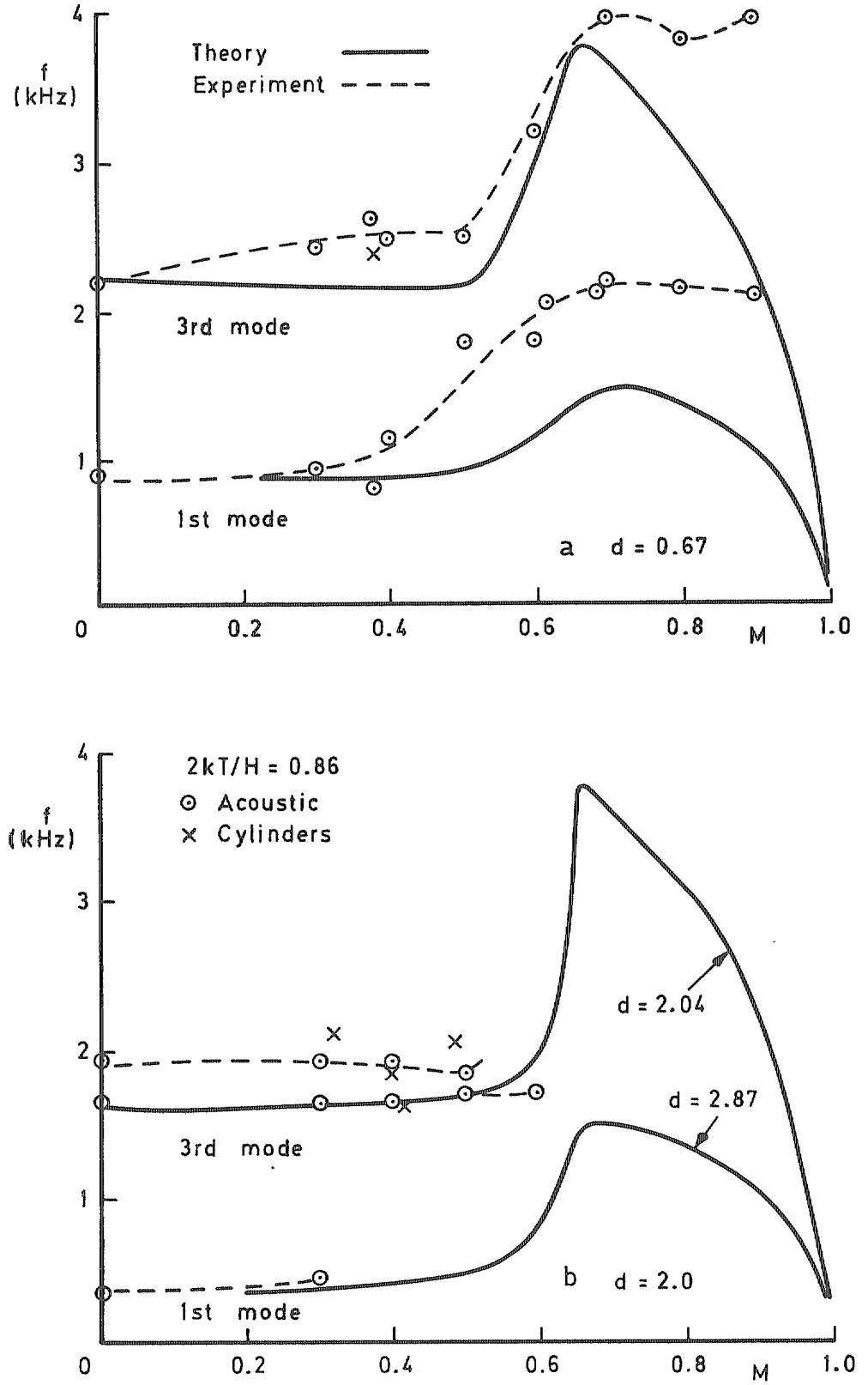

Fig 9 Perforated walls (60° inclined, 6%) — resonance frequencies v Mach number

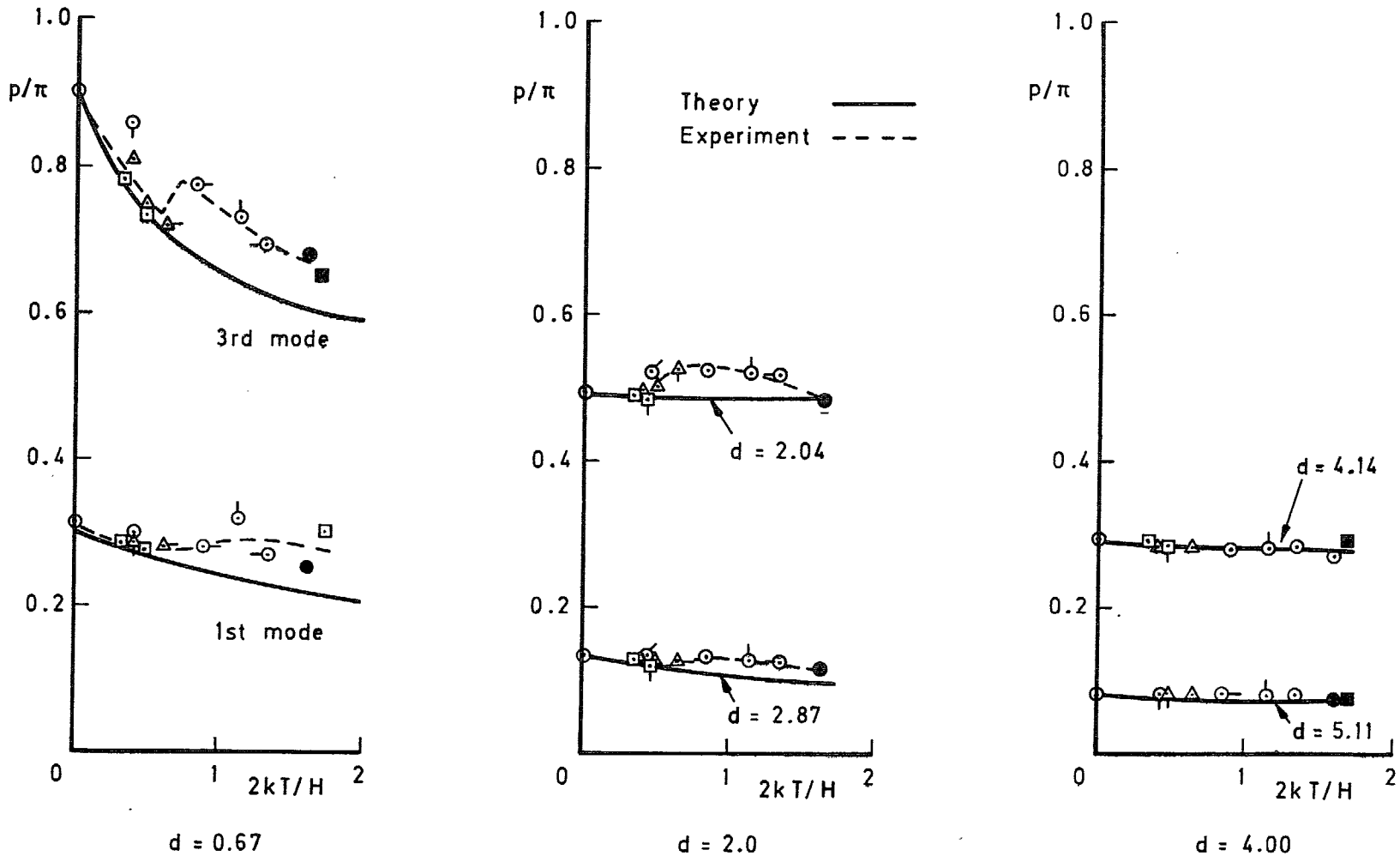

Fig 10 Slotted walls M = 0. Variation of resonance frequency with wall parameter (2 kT/H)

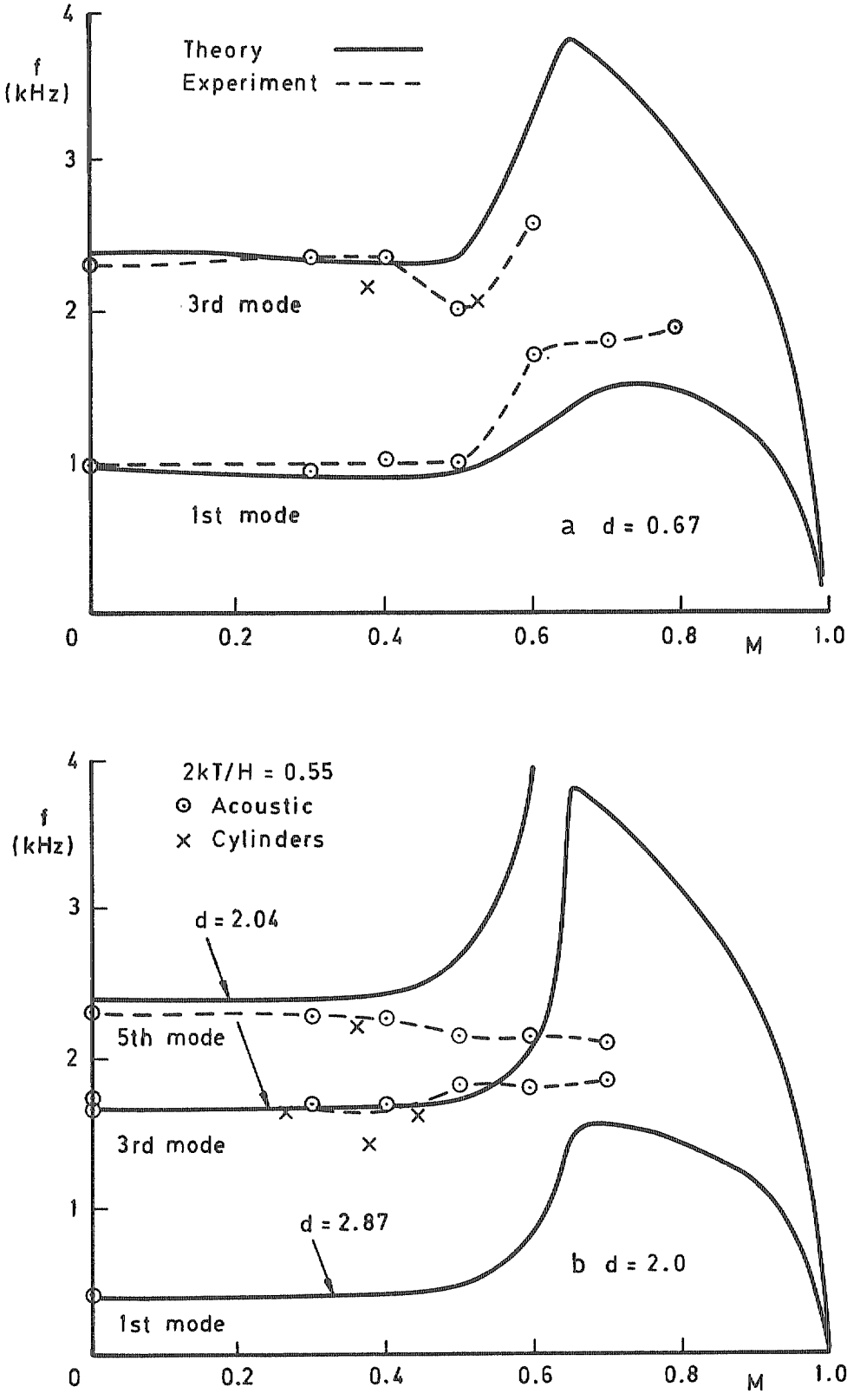

Fig 11a&b Shallow slotted walls — resonance frequencies v Mach number

Fig 12a&b

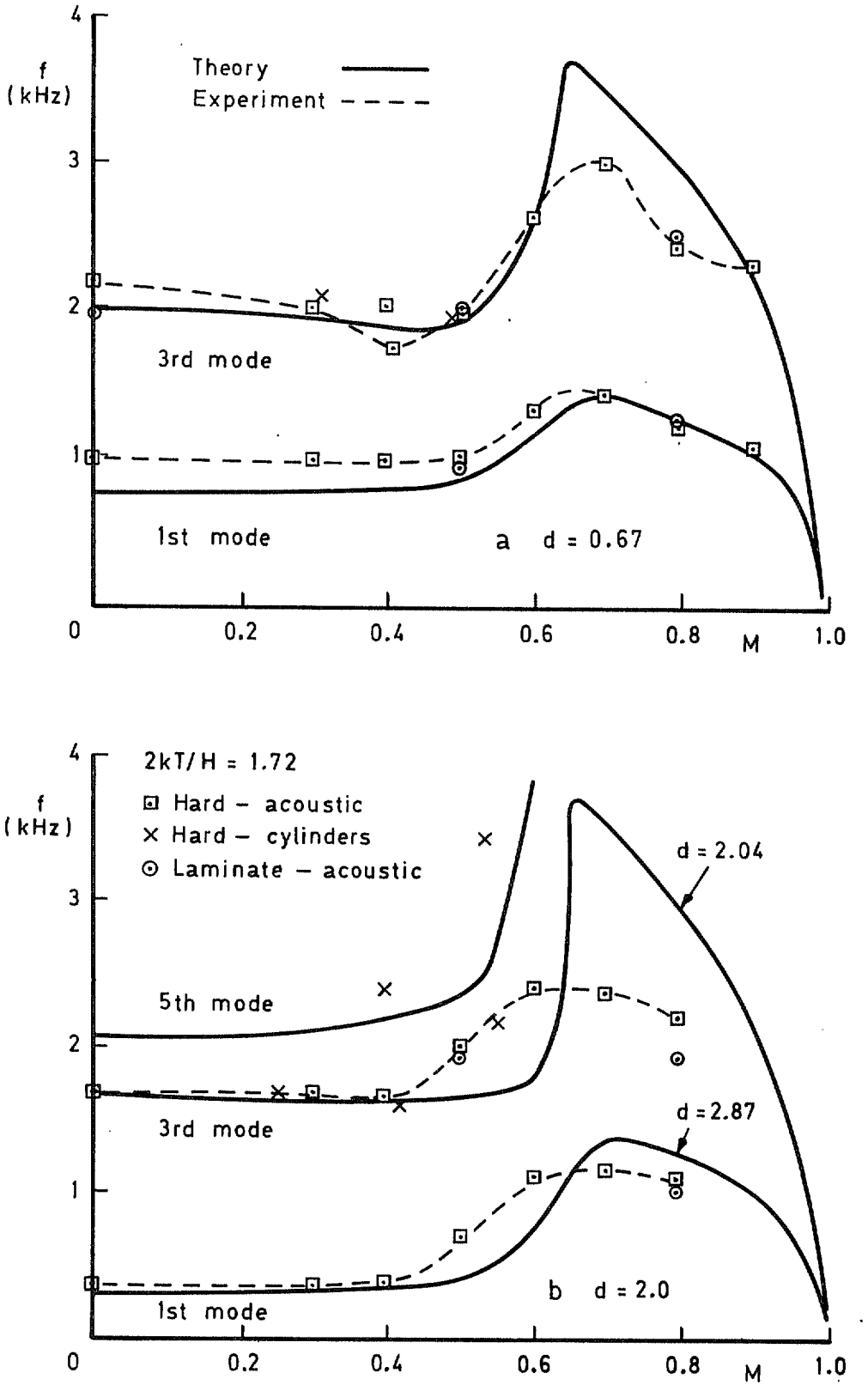

Fig 12a&b Deep slotted walls – resonance frequencies v Mach number

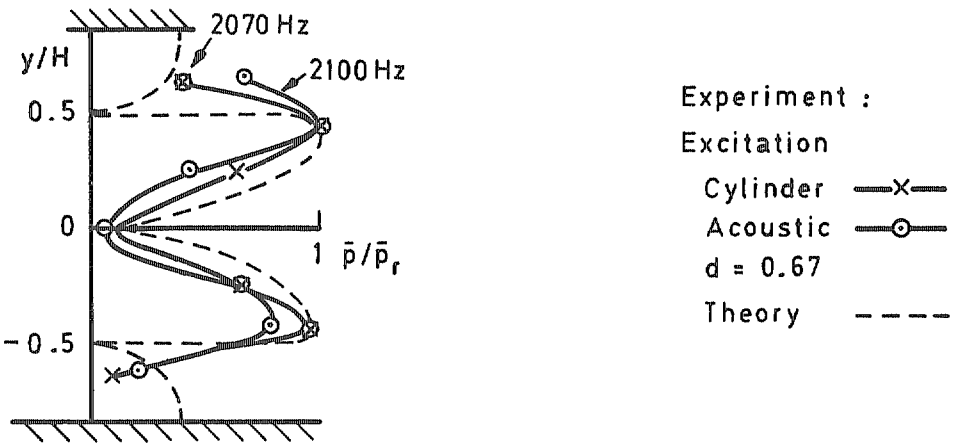

a Deep slotted
M = 0.31, 2kT/H = 1.72

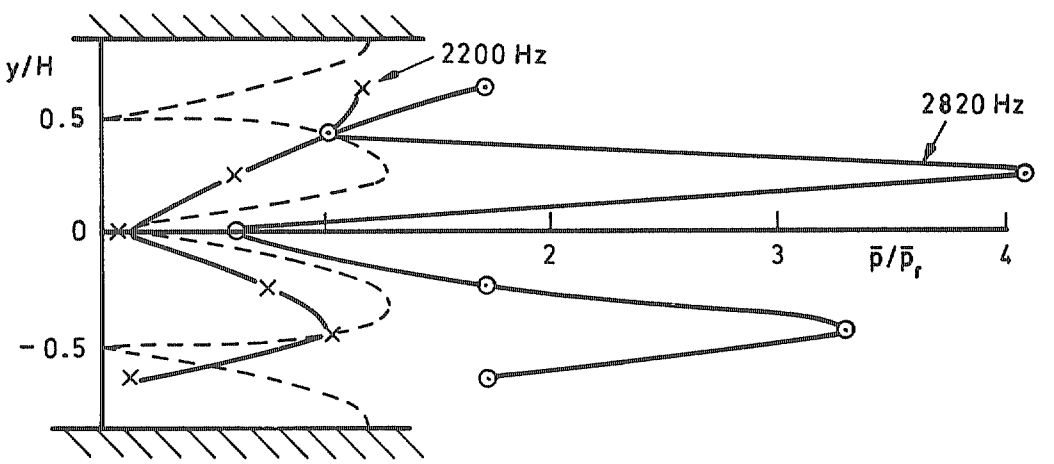

b Perforated normal holes
M = 0.32, 2kT/H = 0.30

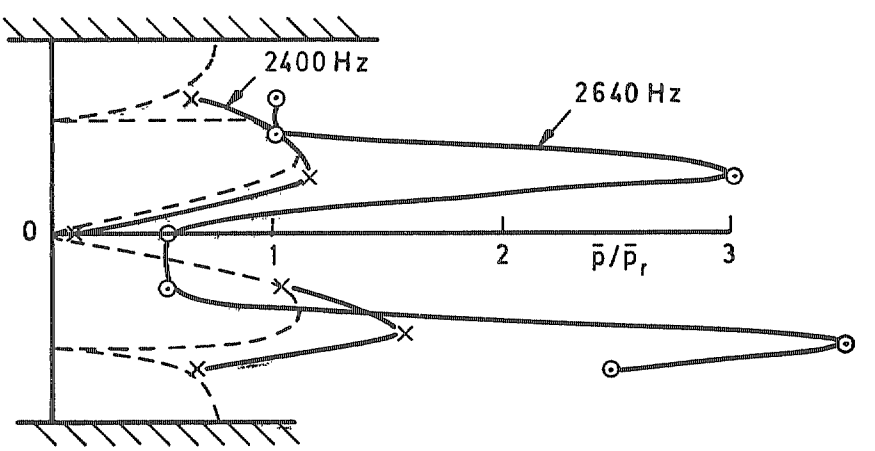

c Perforated 60° inclined holes
M = 0.38, 2kT/H = 0.86

Fig 13a-c Typical third resonance modes

Fig 14

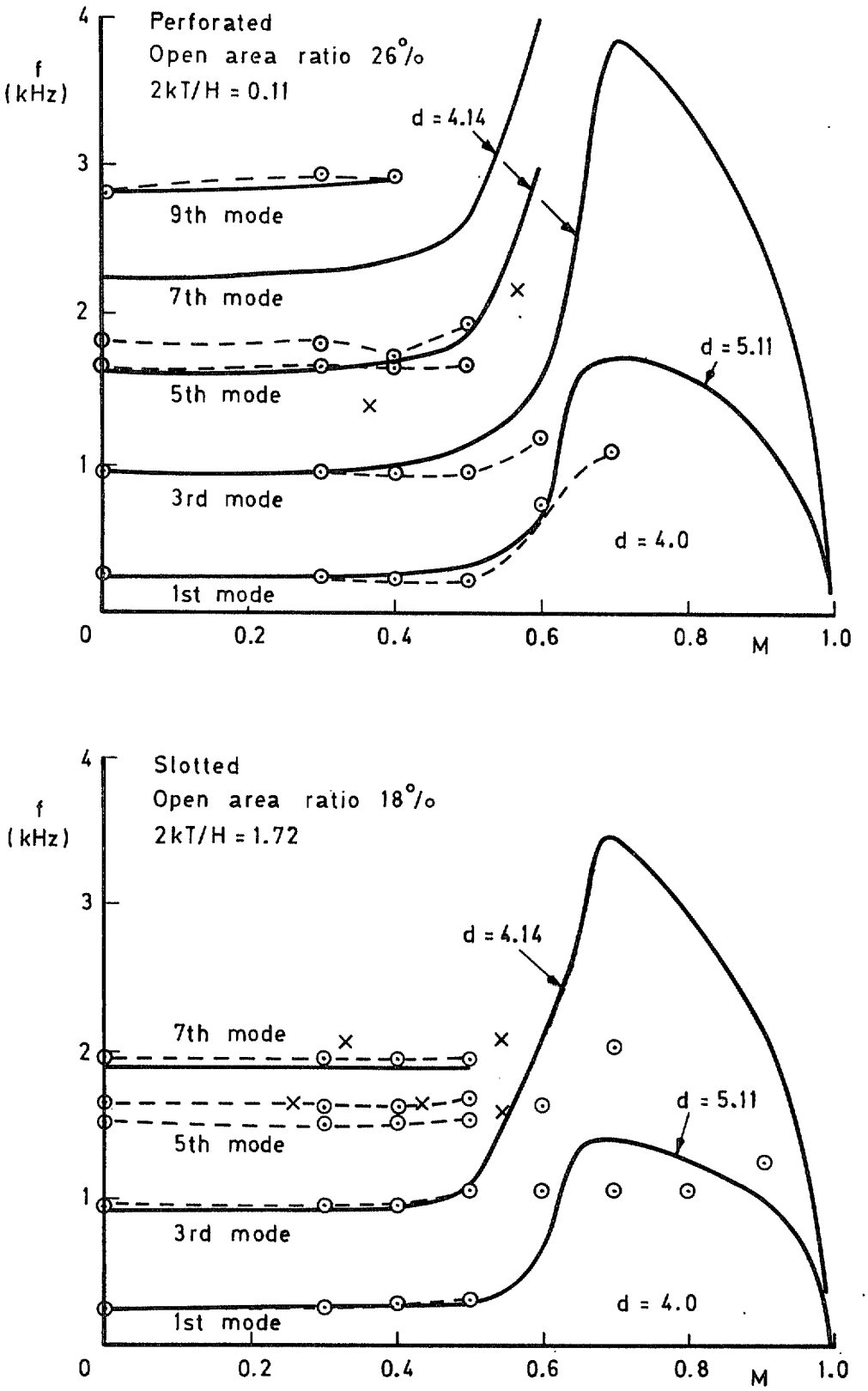

Fig 14 Typical resonance frequencies for a deep plenum chamber

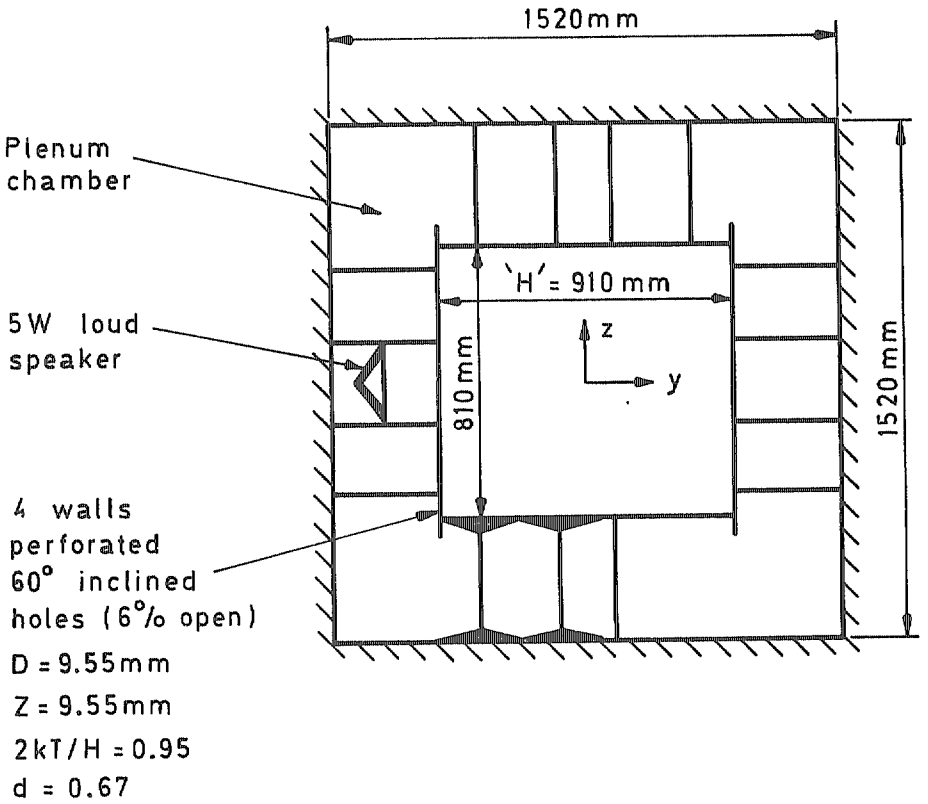

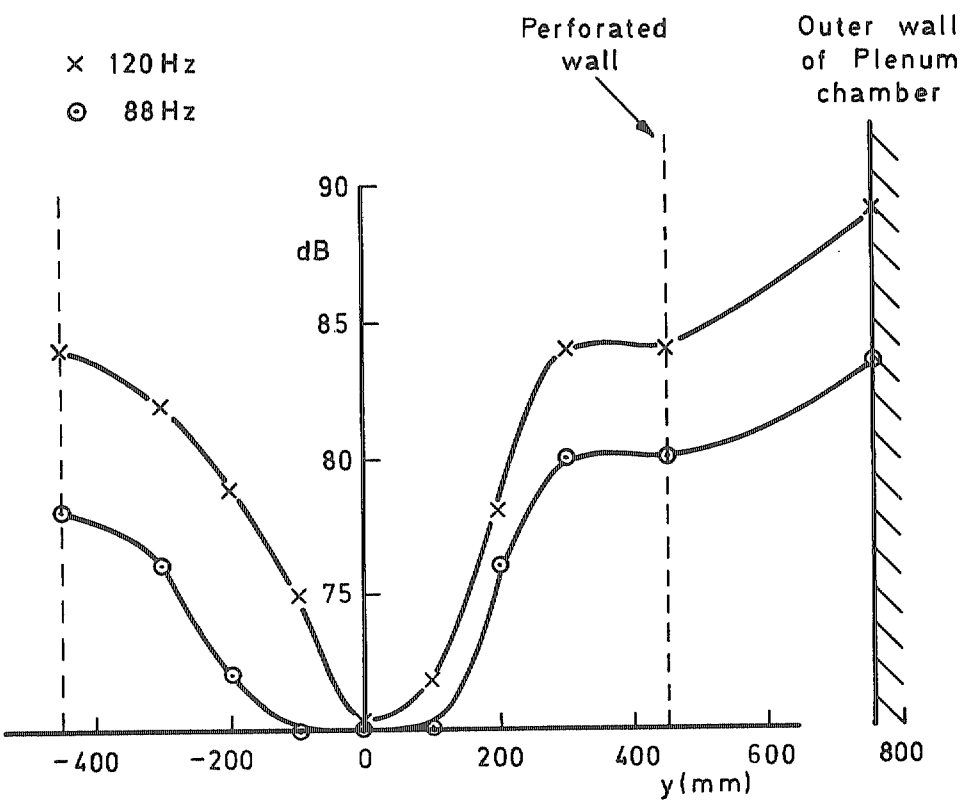

Fig 15 Fundamental modes in perforated working section of RAE 3ft tunnel — M = 0

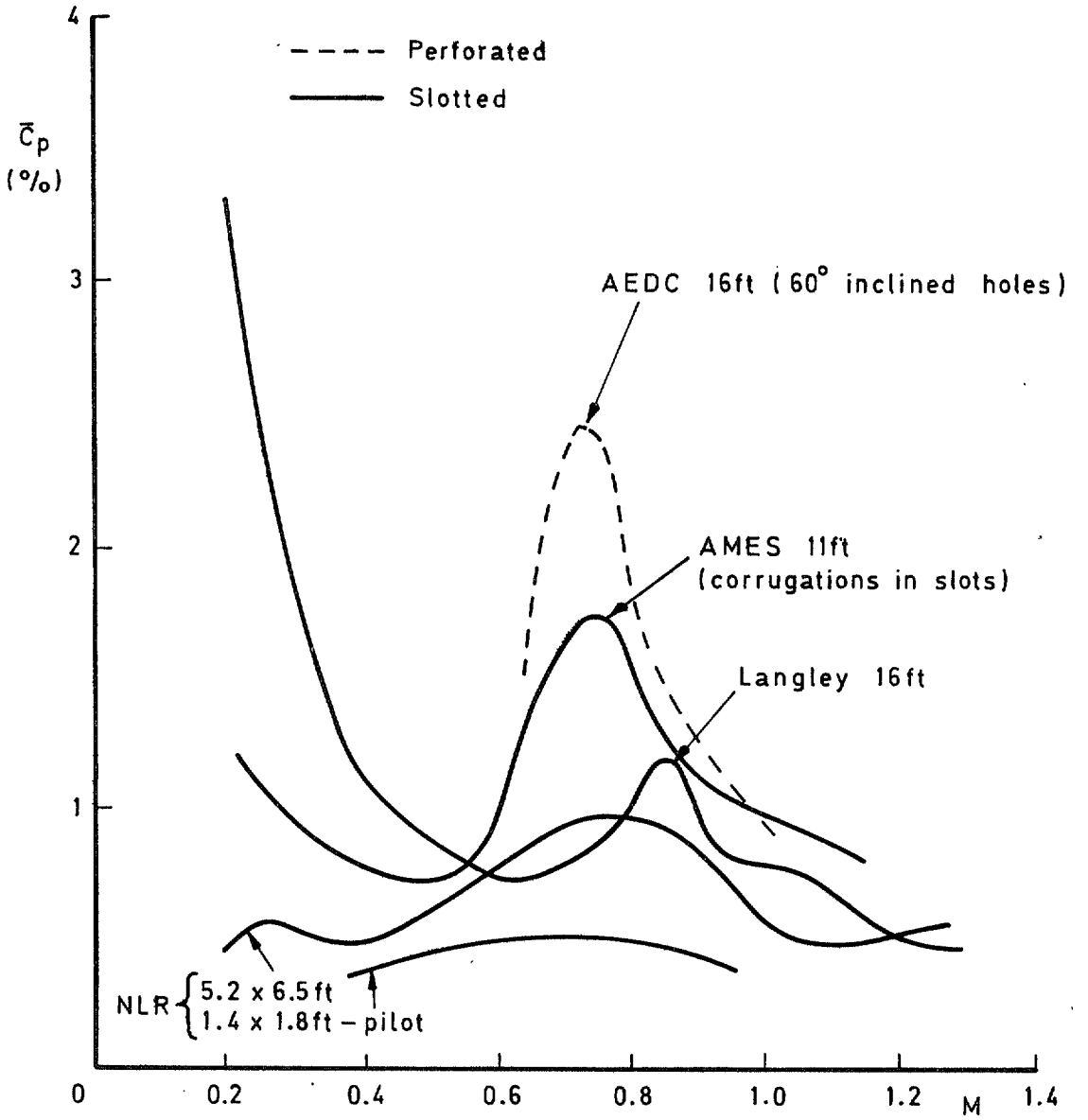

Fig 16 Centre line pressure fluctuations v Mach number for typical transonic tunnels

Printed in England for Her Majesty's Stationery Office by the Royal Aircraft Establishment, Farnborough. Dd.596060 K4 11/79.

First published 1979

HER MAJESTY'S STATIONERY OFFICE

Government Bookshops
49 High Holborn, London WC1V 6HB
13a Castle Street, Edinburgh EH2 3AR
41 The Hayes, Cardiff CF1 1JW
Brazennose Street, Manchester M60 8AS
Southey House, Wine Street, Bristol BS1 2BQ
258 Broad Street, Birmingham B1 2HE
80 Chichester Street, Belfast BT1 4JY

Government Publications are also available through booksellers

R &M No. 3841
ISBN 0 11 471174 7

R &M No. 3841

HMSO